Chapter 4
Potential state of the carbon dynamics in terrestrial ecosystems and the biosphere

4.1. Introduction

Initially, the potential state of carbon cycle in the terrestrial ecosystems is obtained by an iterative model calculation for a sufficiently long period, until ecosystem carbon storage is saturated with carbon, under a given environmental condition. The law of constant final yield (Kira et al. 1953; Shinozaki and Kira, 1961) suggests that a model may attain the equilibrium, independent of initial value and trajectory of biomass (Oikawa, 1985). Ecologically, this potential state is called 'climax' stage of ecosystem succession, where community biomass and soil carbon storage reach their maxima and annual carbon uptake and release are almost balanced, i.e. *NEP* close to zero. In contrast, net primary productivity (*NPP*) is not always at its maximum in this stage. It should be noted that degradation, rendering ecosystems immature again, is an essential process in a majority of natural and artificial ecosystems, because of the occurrence of a variety of disturbances (e.g. wild and anthropogenic fire, pest outbreak, human exploitation, deposition of pollutants, and so on). For example, Bormann and Likens (1979) proposed that the steady state of ecosystem is a dynamic state, rather than a static state, in which death and regeneration of individual trees proceed simultaneously, depicting a mosaic-like distribution pattern. The equilibrium simulation, however, may clarify the indigenous characteristics of carbon budget. Several ecologically interesting issues in relation to productivity and carbon storage can be accessible: regional distribution, latitudinal gradient, seasonal change, biome-to-biome difference, variability within a biome, and C_3 and C_4 plants contribution. The efficiencies of plant productivity at the cost of absorbed radiation energy and transpired water will be addressed, using the outcomes of Sim-CYCLE simulation. Moreover, the role of forest ecosystems in the global carbon cycle deserves investigation, as stated by Dixon et al. (1994). The equilibrium

simulation is also effective for validating the performance of Sim-CYCLE as a reliable simulator of terrestrial ecosystems at the global scale. Especially, mapping of the carbon dynamics with a high spatial resolution model is a timely challenge, which has recently become possible by means of improved computing facilities. However, the success of global simulation is severely determined by the quality of input data, which describe vegetation, soil, climate, and other properties, although considerable efforts are being made to establish the archive of accurate and high-resolution datasets (e.g. IGBP-DIS and Global Map Project). Unhandily, the more mechanistic models become, the more and the finer data are required to perform simulations. The simulation presented in this chapter is one of the latest achievements, making the most of available data to date.

4.2. Methods

Because Sim-CYCLE is a one-dimensional model without any lateral carbon transport and interaction between ecosystems, it is executable at arbitrary spatial scales, from plot scale to global scale. In the global simulation, a high spatial resolution grid system of 0.5° x 0.5° longitude-latitude is selected; this resolution is the upper limit of fineness, restricted by the resolution of input datasets (chiefly of biome map), but may meet the requirement of fine mapping of the terrestrial biosphere. In the 0.5°x 0.5° map (360 rows x 720 columns), area of the grid cell changes with latitude (13.6 to 3077.2 km^2), as approximated by the following:

$$Area = \frac{l_1 + l_2}{2} l_3 \tag{4-1}$$

$$l_1 = \frac{\pi}{180} \cdot \frac{ER \cos(LAT - 0.25)}{\sqrt{1 - EC^2 \sin^2(LAT - 0.25)}} \tag{4-2}$$

$$l_2 = \frac{\pi}{180} \cdot \frac{ER \cos(LAT + 0.25)}{\sqrt{1 - EC^2 \sin^2(LAT + 0.25)}} \tag{4-3}$$

$$l_3 = \frac{\pi}{180} \cdot \frac{ER(1-EC^2)}{\left[1-EC^2 \sin^2(LAT)\right]^{\frac{1}{2}}} \tag{4-4}$$

where ER is the radius of the Earth at the equator (6378.136 km), LAT is the latitude at the center of the grid cell, and EC is the eccentricity of the Earth's orbit (EC^2=0.00669447). Thus, the shape of the Earth was approximated by an ellipsoid, and the shape of grid cell was approximated by a trapezoid, whose length of the upper side is l_1, length of the base is l_2, and height is l_3. The altitude of grid cells (AL) was derived from the ETOPO 5 data (produced by U.S. National Geophysical Data Center in 1983), but the topographic factor was not included in the area calculation. The origin of the grid system is on the cell, 89°45'N – 179°45'W; the grid rows are arrayed from north to south, and grid columns are arrayed from west to east. According to the ETOPO 5 data, the 0.5°x0.5° grid system contains 86,705 of land grid cells whose altitude ranges from 0 to 3186 m above sea level.

An actual biome map by Olson et al. (1983) was adopted for the global simulation. The original map was derived from: (1) patterns of potential vegetation types and their relation to carbon content, and (2) modern areal surveys and intensive biomass data from research sites, partly aided by remote sensing data (Olson et al., 1983). The original biome classification consists of 7 major groups and 44 minor categories (including croplands); in this study, the 44 types were conveniently aggregated into 31 biome types. At this stage, the serious difficulty in the Olson's map, i.e. the confusion of boreal evergreen and deciduous forests, was untangled by referring the Matthews's potential biome map (Matthews, 1983). In consequence, main boreal taiga and northern boreal taiga were respectively divided into evergreen and deciduous types (biomes 9 to 12, in Table 4-1). The resultant 33 biome types were characterized by different parameter values with respect to carbon dynamics; their distribution map is shown in Fig.4-1. For each biome, average environmental factors are listed in Table 4-2, clarifying the difference of their habitat condition.

One of the most remarkable achievements of plant ecophysiology during the recent decades is the discovery of C_4 photosynthetic pathway (ca. 1954-1967; Hatch, 1997), which

uses different primary enzyme (i.e. phosphoenolpyruvate carboxylase) from normal C_3 pathway (ribulose-1,5-bisphosphate carbonxylase/oxygenase) to capture atmospheric CO_2. As listed in Table 2-1, C_3 and C_4 photosynthetic pathways are distinctive in various points, and then it is very important to determine the composition of C_3 and C_4 plants for simulation studies of carbon dynamics, biome distribution, and atmosphere-biosphere interactions. Because C_4 plants take herbaceous growth forms (both mono- and di-cotyledonous), their distribution is restricted to grasslands (biomes 14 to 19) and deserts (biomes 27 and 28). Unfortunately, there is no general model to estimate how much C_4 plants dominate the plot, mainly because of the diversity of C_4 plants (about 10,000 species) and the insufficiency of field survey. Ehleringer (1978) and Ehleringer et al. (1997) suggest that the difference in photosynthetic light-use efficiency (i.e. QE in Eq. 2-39) between C_3 and C_4 plants is most strongly relevant to the difference in carbon gain by these plants, but there remains a great uncertainty in applying the hypothesis to the global scale. Empirically, dominance of C_4 plants is apparently related to site latitude (French, 1979; Sage et al., 1999), probably via some critical temperature factors (Teeri and Stowe, 1976), such that C_4 plants predominate in lower latitudes. Accordingly, areal composition of C_4 plants (F_{C4}, in % area cover) in grasslands and deserts was formulated as follows (Fig. 4-2):

$$F_{C4} = \begin{cases} 0 & (LAT \geq 50^\circ) \\ 227.36 - 4.5704LAT & (49^\circ \geq LAT \geq 30^\circ) \\ 95 & (LAT \leq 29^\circ) \end{cases} \tag{4-5}$$

Equation 4-5 suggests that the crossover latitude (where C_3 and C_4 plants predominate evenly) is about 39°N/S. Based on Eqs. 4-1 and 4-5, areal occupancy by C_3 and C_4 plants was estimated as 103.4 and 43.1 x 10^6 km^2, respectively (C_4 plants occur in 18,564 grid cells). At the present stage, longitudinal change in F_{C4} was remained for the future study, and biome distribution and C_3/C_4 composition were assumed to be static, i.e. independent of ecosystem

succession and climatic variation. As to soil properties used in the water budget subscheme, water holding capacity and rooting depth were derived from Bouwman et al. (1993) and Zobler (1986), respectively. These soil datasets have originally a spatial resolution of 1° x 1° longitude-latitude, and then were simply interpolated into 0.5° x 0.5° longitude-latitude. The long-term mean climate data was created by the author (cf. Chapter 2), by averaging and interpolating the dataset by U.S. National Centers for Environment Prediction (NCEP) and U.S. National Center for Atmospheric Research (NCAR) (Kalnay et al., 1996), from 1961 to 1998. Finally, atmospheric CO_2 concentration was assumed as 352.7 ppmv, i.e. the level in 1990 (Keeling and Whorf, 2000). The equilibrium state was attained in a similar manner to the plot-scale, such that simulation was launched from the juvenile stage (0.1 Mg C ha^{-1} for each compartment) and continued until reaching the stable state (*NEP*<0.0001 Mg C ha^{-1} yr^{-1}). Based on the plot-scale simulation, ecophysiological parameters related to carbon dynamics were determined as listed in Table 4-3.

4.3. Results

4.3.1. Overview of carbon fluxes

At the equilibrium state, global annual GPP and *NPP* was estimated as 147.5 and 61.8 Pg C yr^{-1}(Fig.4-3); then *NPP* accounted for 41.9 % of *GPP*. In the total *NPP*, natural biomes (types 1 to 28) contributed 52.8 Pg C yr^{-1} (85.4%), and the residual 9.0 Pg C yr^{-1} was by agricultural ecosystems (types 29 to 32). As shown in Fig. 4-4, annual *NPP* over the terrestrial biosphere was highly heterogeneous, ranging from 0 in deserts and frigid regions to 14 Mg C ha^{-1} yr^{-1} in tropical humid regions. At the global scale, CO_2 efflux from soil surface (so-called soil respiration) was estimated as 92.3 Pg C yr^{-1}, of which 33.9 % was from root respiration, and 66.1 % was from soil decomposition, or heterotrophic respiration.

4.3.2. Overview of carbon storage

In the simulation exercise, the equilibrium biospheric carbon storage reached as large as 2149.8 Pg C, of which 30.1 % (646.1 Pg C) was attributable to plant biomass *WP* and

residual 69.9 % (1503.7 Pg C) was to soil organic matter *WS* (Figs. 4-3 and 4-5). In other words, only 25.4 % existed aboveground as plant leaves and stems, and the majority of carbon was stored underground as roots and soil organic matter. Among the plant compartments, stems were the largest one, containing carbon as much as 524.6 Pg (81.2 % of plant biomass), and secondarily roots stored 99.8 Pg C. The assimilative organ, or leaves, accounted only for 21.7 Pg C (3.36 % of plant biomass), being astonishingly small quantity in the light of their essential activity in terrestrial ecosystems. Total leaf area was estimated as 340.5 x 10^6 km^2, i.e. average *LAI* was 2.3. Plant aboveground/belowground biomass ratio was 5.47, while ecosystem aboveground/belowground ratio was 0.34. The mineral soil compartment (WS_H in Fig. 4-3) stored a huge amount of biogeochemically stable carbon (1430.1 Pg C), rather than litter one WS_L (73.6 Pg C). As litterfall of 61.0 Pg C was shed from plant to soil, mean resident time of litter carbon was 1.2 years, which were significantly shorter then the time of mineral soil of 40.1 years.

4.3.3. Inter-biome comparison of productivity and carbon storage

The 32 of biome types (excluding biome 33, ice sheet) differed substantially in their carbon storage and *NPP* (Fig. 4-6, Tables 4-4 and 4-5). *NPP* ranged from 0.6±0.6 Mg C ha^{-1} yr^{-1} in non-polar sand desert (biome 28) to 10.7±2.2 Mg C yr^{-1} in tropical rain forest (biome 1). Apparently, forest ecosystems had higher *NPP* than grasslands, tundras, and deserts, and there was an obvious gradient in *NPP* from tropical to boreal forests (Fig. 4-6, biomes 1 to 12). The differences in carbon storage between forest and non-forest ecosystems were also evident, for both plant carbon and soil carbon storage. However, cooler rangelands, i.e. Tibetan and Siberian fields (biome 19) and tundra ecosystems (biomes 20 and 21) had as high soil carbon storage (over 200 Mg C ha^{-1}) as productive forest ecosystems. The frequency distribution of *NPP* (Fig. 4-7a) depicts an L-type distribution; a large number of infertile grid cells (over 12,000) were occupied by non-productive tundra and desert ecosystems. Both of grassland and forest ecosystems had a wide range of distribution and two peaks; for forests, there are those around 5 and 11 Mg C ha^{-1} yr^{-1}; and for grasslands, peaks around 1 and 8 Mg C ha^{-1} yr^{-1},

respectively. Interestingly, around 8 Mg C ha^{-1} yr^{-1}, the peak of grassland *NPP* compensated a trough of forest *NPP* distribution.

4.3.4. Time to reach equilibrium

The average simulation time until reaching an equilibrium was 517.8 years of repetition, with a broad range of inter-biome difference from 156 years of paddy field (biome 29) to 1156 years of northern evergreen taiga and cool rangelands (biomes 12 and 20) (Table 4-5). The differences were likely to be related to the magnitude of soil organic carbon pool and the activity of carbon flow in the ecosystem (discussed later). In spite of a large amount of biomass storage, tropical rain forests (biome 1) took shorter time to reach the equilibrium (280$\pm$16 years), probably due to their active carbon dynamics of the soil compartments. This is very contrastive to the inactive carbon dynamics in boreal forests (biomes 7 to 12), which took at least 550$\pm$242 years for equilibration. Interestingly, grassland ecosystems were not always equilibrated in shorter times (500 to 800 years) than forest ecosystems, because lower decomposition rates due to moisture deficit resulted in a slow turnover of soil organic carbon. The inactive soil carbon dynamics was also evident in tundra ecosystems (about 1000 years for equilibration), but owing to another mechanism, that is, their lower soil temperature.

4.3.5. Latitudinal distribution

Table 4-6 summarizes the estimated carbon dynamics (and other properties related to water and radiation) for every 10-degree latitudinal zone. As shown in Table 4-4 and Fig. 4-8, the latitudinal distribution of carbon storage had two peaks, one around the equator and another around 60°N. The equatorial one consists chiefly of biomass of tropical forests, and the boreal one was ascribable to soil organic carbon in boreal forests and tundras (these zones contained larger land area; cf. Table 4-4). In other words, northern subtropical zones (10 to 30° N) had smaller carbon storage, because they were dominated by arid biomes which had low productivity and biomass storage. For example, average *LAI* in 20 to 40°N (1.7 to 1.8) was apparently smaller than its upper and lower latitudes (2.0 to 4.5, cf. Table 4-3).

4.3.6. Seasonal change

The seasonal change in the global carbon dynamics was comprehensively exemplified by comparing with two contrastive months, i.e. February and July (Fig. 4-9). In one year, *GPP* changed two-fold, from 8.8 Pg C mon^{-1} in February to 17.9 Pg C mon^{-1} in July, driven by the seasonality in temperate and boreal biomes in the Northern Hemisphere (Fig. 4-10). Plant respiration *AR* increased in summer of the Northern Hemisphere (from 5.4 Pg C mon^{-1} in February to 9.8 Pg C mon^{-1} in July); this was firstly attributable to growth respiration change (from 2.8 Pg C mon^{-1} in February to 6.1 Pg C mon^{-1} in July) and secondarily to maintenance respiration change (from 2.6 Pg C mon^{-1} in February to 3.7 Pg C mon^{-1} in July). Consequently, *NPP* changed from 3.4 Pg C mon^{-1} in February to 8.1 Pg C mon^{-1} in July (Fig. 4-11 and Table 4-5). Because soil heterotrophic respiration *HR* varied from 3.6 Pg C mon^{-1} in February to 7.2 Pg C mon^{-1} in July, *NEP* had a wide amplitude of as large as 2.2 Pg C, from +1.4 Pg C mon^{-1} in June and –0.8 Pg C mon^{-1} in October (Fig. 4-12). The seasonal change in *NEP* would be clarified by introducing a new index, total net exchange *TNE*, defined as follows:

$$TNE = \sum_{i=1}^{12} |NEP_i| \tag{4-6}$$

where plain brackets | | denotes an absolute value, and NEP_i is the *NEP* in the *i*th month. Thus, *TNE* is more deeply related to the seasonal change in atmospheric CO_2 concentration, on which terrestrial carbon budget exerts an effect cumulatively through months. Zonal *TNE*s in Table 4-6 indicate that the northern high region (40° to 70°N), which has *TNE* of 7.2 Pg C yr^{-1}, would contribute considerably to the seasonal oscillation of atmospheric CO_2. Similarly, it can be seen from Fig. 4-13 that carbon dynamics changed with latitude; seasonal *NPP* variations between above and below 20°N are very contrastive. The seasonality in climatic conditions increases abruptly around the latitude; e.g. mean annual range of temperature is 2.3°C in 0-

10°N, 8.4°C in 10-20°N, and 16.8°C in 20-30°N. The seasonal change in *NPP* was partly related to the phenological change in vegetation activity, as exemplified by *LAI* variation (Fig. 4-14).

4.3.7. Additional regional aspects

Comparison between the Northern Hemisphere and the Southern Hemisphere

Figures 4-15a and 4-15b summarize the carbon dynamics in the Northern Hemisphere (NH) and the Southern Hemisphere (SH), respectively. The NH exhibits two-fold *NPP* than the SH, because of the approximately two-fold land area (cf. Table 4-4), whereas the NH contains three-fold carbon storage than the SH. The excessive difference in carbon storage between the NH and SH is attributable to the large difference in soil carbon storage, because the SH lacks boreal forests and tundras at all (cf. Fig. 4-1), which have a great amount of soil carbon storage around 50 to 70°N (cf. Table 4-4). The total *TNE* in the NH is 13.8 Pg C yr^{-1}, while that of the SH is only 3.0 Pg C yr^{-1}; this difference may be related to the difference in seasonal amplitude and phase of atmospheric CO_2 concentration between NH and SH (for *NPP*, see Fig. 4-13b).

Regional carbon dynamics: Monsoon Asia and Siberia

Figure 4-16 exemplifies the carbon dynamics in two representative, contrastive regions: Monsoon Asia (50°N to 10°S, 60 to 180°E, 20.9 x 10^6 km^2) which contains a large area of tropical forests (biomes 1 to 3), and Siberia (50 to 90°N, 60°E to 170°W, 16.7 x 10^6 km^2) which is mostly occupied by boreal forests (biomes 8 to 12) and tundras (biomes 21 and 22). In spite of the smaller land area and lower *NPP*, Siberia (*WE*=489.7 Pg C) accumulated 42% more carbon than Monsoon Asia (*WE*=343.6 Pg C). The two regions differ remarkably in their soil to plant carbon storage ratio (*WP/WS*): 0.61 of Monsoon Asia and 0.16 of Siberia. A large area of Monsoon Asia is under the monsoon climate, with apparent rainy and drought seasons, and therefore the difference in seasonality in the two regions was evident not only in quantity but also in quality (cf. LPF site and BLF site in Chapter 3).

4.3.8. C_3/C_4 species

As shown in Figure 4-17, C_4 plants contributed significantly to the global carbon dynamics, such that assimilated a notable amount of carbon through their characteristic photosynthetic pathway: 38.1 Pg C yr^{-1} of *GPP* (25.8 % of the global total) and 12.5 Pg C yr^{-1} of *NPP* (20.2 % of the global total). This high productivity is contrastive to their tiny biomass. However, soil organic carbon supplied by C_4 plants occupied 155.8 Pg C, or 10.3 % of global soil matter; this quantity would have a significant meaning in considering the budget of carbon isotopes (^{12}C and ^{13}C), because C_4 plants have generally higher $\delta^{13}C$ values (-7 to -15 ‰) than C_3 plants (-20 to -35 ‰) (Jones, 1992). As expected from their geographical distribution, C_4 plants had larger contribution to zonal carbon cycle in lower latitudes; e.g. in 20 to 30°S (including African savannas and Australian deserts), C_4 plants performed as much as 47.5 % of zonal *NPP* (cf. Fig. 4-8 and Table 4-3).

4.3.9. The role of forests

The forest biomes, which cover 37.3 x 10^6 km^2 of land area, were estimated to be an important component of global carbon cycle (Fig. 4-18). The annual forest *NPP* was estimated as 28.4 Pg C yr^{-1}, which is about a half of the global biospheric one (i.e. 61.8 Pg C yr^{-1}). Their estimated biomass, 511.3 Pg C, may occupy 77 % of the global biospheric one (646 Pg C), and the estimated soil organic carbon storage, 658.4 Pg C, may occupy 44 % of the global biospheric one (1504 Pg C). Their average carbon densities were 125.5 and 181.8 Mg C ha^{-1} for plant and soil carbon storage, both of which are significantly larger than non-forest ones, 12.2 Mg C ha^{-1} and 79.5 Mg C ha^{-1}, respectively. Among the forest biomes, tropical forests (biomes 1 to 3) had the largest contribution to *NPP*, attributable to their high productivity (Table 4-5). In the tropical forests, plant carbon storage (*WP*=308.2 Pg C) was considerably larger than soil carbon storage (*WS*=159.2 Pg C). These aspects were very contrastive to those of boreal forests, which showed low productivity and large soil carbon storage (*WS*=315.5 Pg C). Temperate forests (biomes 4 to 7) had moderate productivity and carbon storage (*WE*=294 Pg C), but it is noteworthy that their estimations may not quantify

their potential property, because their considerable area should have been converted to croplands.

Figure 4-7b shows that annual *NPP* of forest cells had two peaks in their frequency distribution: one around 5 Mg C ha^{-1} yr^{-1} composed mainly of boreal forests and another around 11 Mg C ha^{-1} yr^{-1} of tropical forests. Between the two peaks, there is a large gap which would be filled by temperate forests in case of the potential vegetation. We could see a similar pattern in the latitudinal *NPP* distribution (Fig. 4-8), in which forests in low and northern-high latitudes had peaks, respectively.

4.3.10. Radiation and water use efficiencies

When carbon cycle reached the equilibrium, the optimum leaf area index LAI_{OPT} was realized and then water and radiation budget was also at the steady state. Average annual precipitation was 770.3 mm, of which 96.2 mm were lost by evaporation from soil surface, 331.4 mm by transpiration from canopy, and 341.6 mm by runoff. Average soil moisture content was 617.8 mm, with a wide range of intra-biome variation ranging from 81.5 mm of sand deserts (biome 28) to 1733 mm of cool bogs (biome 24). Average PAR irradiance at midday ($PPFD_{MD}$) was 1146.3 μmol photons m^{-2} s^{-1}, and 136.7 x 10^{18} J (i.e. 2.35 GJ m^{-2} yr^{-1}) was absorbed by vegetation. The fraction of absorbed PAR ranged from 0.9 in tropical and temperate broad-leaved forests (biomes 1 and 5) to 0.1 in sand deserts.

At the global scale, efficiencies of photosynthetic production at the cost of transpired water and absorbed radiation energy (*WUE* of Eq. 2-71 and *RUE* of Eq. 2-72) were estimated as 1.26 g C kg^{-1} H_2O and 0.396 g C MJ^{-1}, respectively. *WUE* and *RUE* were not homogeneous over the biosphere (Fig. 4-19). Apparently, arid grasslands and deserts (e.g. Sahara and central Australia) show higher *WUE*s (2 to 3 g C kg^{-1} H_2O) than forest ecosystems. In contrast, forest ecosystems (especially tropical rain forests) show higher *RUE*s (0.6 to 0.8 g C MJ^{-1}, cf. Table 4-6). These differences among biome types would have a relevance to canopy architecture, such that forests with higher *LAI* absorbed more radiation and performed active phosynthetic production, at the cost of larger water loss by transpiration.

4.4. Discussion

4.4.1. Comparison with other model studies

The global carbon dynamics estimated by Sim-CYCLE, mentioned in the previous sections, should be validated by comparing with other estimations. Three empirical models on *NPP* estimation were employed:

(1) Chikugo model This model was developed by Uchijima and Seino (1985), for estimating the potential primary productivity in Japan and the world, from the point of agrometeorological view:

$$NPP = 0.45\left[0.29\ \exp\left(-0.216\ RDI^2\right)\right] RN \tag{4-7}$$

where *RN* is the annual net radiation, and *RDI* is the radiative dryness index defined as *RN/LH•PR* (*LH* is the latent heat of vaporization, and *PR* is the annual precipitation). These climatic data were derived from a similar dataset to Sim-CYCLE, i.e. the NCEP/NCAR-reanalysis.

(2) Miami model This model was developed by Lieth (1975), based on a large amount of the IBP field data, in order to empirically estimate the potential productivity of the biosphere:

$$NPP = \min\left\{NPP_{TEM}, NPP_{PRE}\right\} \tag{4-8a}$$

$$NPP_{TEM} = \frac{13.5}{1+\exp\left(1.315-0.119\ TA\right)} \tag{4-8b}$$

$$NPP_{PRE} = 13.5\left[1-\exp\left(-0.000664\ PR\right)\right] \tag{4-8c}$$

where NPP_{TEM} and NPP_{PRE} are respectively the values of potential productivity limited by temperature and water condition, and *TA* is the annual mean air temperature, and *PR* is the annual precipitation (from NCEP/NCAR-reanalysis).

(3) Box's model This model was developed by Box et al. (1989), who realted remotely sensed Normalized Difference Vegetation Index (*NDVI*) to *NPP*:

$$NPP = 8.2556 \ \ln\left(\frac{0.4}{0.4 - NDVI}\right) \tag{4-9}$$

In this study, *NDVI* values were derived from the Maximum Vegetation Index data by U.S. National Oceanographic and Atmospheric Administration (NOAA), from 1983 to 1992.

These three empirical models estimated total *NPP*: 60.8 Pg C yr^{-1} by Chikugo model, 57.1 Pg C yr^{-1} by Miami model, and 60.8 Pg C yr^{-1} by Box model, being adequately close to that of Sim-CYCLE (61.8 Pg C yr^{-1}). Figure 4-20 shows that a point-by-point comparison between Sim-CYCLE and other three models resulted in satisfactory agreement; correlation coefficient (r) was as high as 0.753 to 0.841. This intercomparison of models may support that Sim-CYCLE captured a moderate feature of global carbon cycle, although such other features as carbon storage and seasonal variability were not scrutinized here.

Dixon et al. (1994) presented another estimation of the carbon budget of global forest ecosystems, based on a large amount of empirical and inventory data. Their analysis includes some open forests, leading to a broader forest area at present (41.7 x 10^6 km^2) than the Sim-CYCLE one (37.3 x 10^6 km^2). They suggest that carbon stocks in forest plant and soil are 359 and 787 Pg C, respectively. The average carbon density of biomass and soil organic matter are estimated as 86 and 189 Mg C ha^{-1}, respectively. Then, soil carbon density estimated by Sim-CYCLE (181.8 Mg C ha^{-1}) agrees well with their estimation, while the plant biomass (125.5 Mg C ha^{-1}) is about 40 % larger than their value. Apparently, this difference of biomass density is attributable to the difference of the definition of forest ecosystem (i.e. closed and open forests), and to the assumption of equilibrium state in the present study. Therefore, it is expected that including the effect of human management and wildfire in our simulation analysis may reduce the difference, although a potential carbon budget is often more suggestive than the actual one, when one considers the biotic feedbacks to the global

environmental change in the past and the future.

4.4.2. A caveat on spatial resolution

Viewing locally, the spatial resolution of 0.5°x 0.5° (about 55 km) may be insufficient to retrieve the heterogeneity seen at a landscape level, but running the model at a finer resolution (e.g. 1 km mesh) demands about 3000 times of computational exertion, making it impossible to perform a global simulation. Therefore, this problem should be solved by so-called 'nesting' method: using multiple models at different positions in spatial-scale hierarchy from single leaf to the biosphere (Ehleringer and Field, 1991; Jarvis, 1995).

Table 4-1. Classification, cell number, and area of 33 biome types in Sim-CYCLE simulation.

No.	Biome type	C_3	C_4	Grid-cell frequency Total	N90-60	N60-30	N30-0	S0-30	S30-60	S60-90	Area (10^6 km^2)
0	Water			172495	27734	21575	30636	33339	40975	18236	362.7
1	Tropical and subtropical evergreen forest	O		3430	0	0	1471	1959	0	0	10.5
2	Tropical montane forest	O		394	0	0	257	137	0	0	1.2
3	Tropical and subtropical dry forest	O		1584	0	0	470	1113	1	0	4.7
4	Mid latitude mixed woods	O		1589	145	930	384	13	117	0	3.5
5	Mid latitude broad-leaved forest	O		676	22	487	21	9	137	0	1.5
6	Semiarid wood or low forest	O		324	0	3	0	277	44	0	0.9
7	Coniferous forest	O		1719	26	1636	53	0	4	0	3.5
8	Southern taiga	O		903	32	871	0	0	0	0	1.6
9	Main boreal taiga (evergreen)	O		2238	1488	748	2	0	0	0	3.4
10	Main boreal taiga (deciduous)	O		1341	686	655	0	0	0	0	2.1
11	Northern taiga (evergreen)	O		1898	1397	501	0	0	0	0	2.7
12	Northern taiga (deciduous)	O		1277	1220	57	0	0	0	0	1.6
	total forests			17373	5016	5888	2658	3508	303	0	37.3
13	Second growth woods	O		2232	21	1586	275	206	144	0	5.2
14	Second growth fields	O	O	1680	11	1003	292	314	60	0	4.1
15	Succulent and thorn woods	O	O	1350	0	0	505	770	75	0	4.0
16	Tropical savanna, woodland	O	O	2229	0	0	1352	876	1	0	6.7
17	Mediterranean-type dry woods	O	O	1374	0	548	102	361	363	0	3.6
18	Heath and Moorland	O	O	72	0	45	0	7	20	0	0.1
19	Warm or hot shrub and grassland	O	O	6400	2	2204	2034	1810	350	0	17.3
	total grasslands			15337	34	5386	4560	4344	1013	0	41.0
20	Tibetan meadow, Siberian highland	O		425	191	200	34	0	0	0	0.8
21	Tundra	O		7592	6116	1264	95	80	37	0	9.9
22	Wooded tundra	O		1236	885	334	10	1	6	0	1.7
23	Warm or hot wetlands	O		546	7	62	182	275	20	0	1.6
24	Cool bog and mire	O		576	152	411	2	9	2	0	1.0
25	Shore and hinterlands	O		403	10	171	107	48	67	0	1.0
	total tundras			10778	7361	2442	430	413	132	0	16.0
26	Cool semi-desert scrub	O		930	0	612	2	1	315	0	2.0
27	Non-polar desert	O	O	4070	0	1161	2343	533	33	0	11.1
28	Non-polar sand desert	O	O	1930	0	481	1038	402	9	0	5.2
	total deserts			6930	0	2254	3383	936	357	0	18.3
29	Paddyland	O		697	0	164	490	42	1	0	2.0
30	Cool croplands	O		1477	18	1423	15	15	6	0	3.0
31	Warm croplands	O		5553	42	3724	875	551	361	0	13.2
32	Irrigated	O		627	26	344	153	52	52	0	1.6
	total croplands			8354	86	5655	1533	660	420	0	19.7
33	Antarctica			27933	2969	0	0	0	0	24964	15.1
	total lands			86705	15466	21625	12564	9861	2225	24964	147.4
	total earth			259200	43200	43200	43200	43200	43200	43200	510.1

Table 4-2. Average climate condition and radiation and hydrological environment in 32 biomes.

	Anneal climate condition				Radiation		Hydrology (mm yr^{-1})			
	Temperature (°C)		Precipitation (mm)		Down. (W m^{-2})	Absorbed (GJ m^{-2} yr^{-1})	Evapo.	Transp.	Runoff	Soil W
No.	Av.	SD	Av.	SD	Av.	Av.	Av.	Av.	Av.	Av.
0	16.1	11.9	1050.6	708.5	202.3	-	-	-	-	-
1	23.4	2.0	2243.6	788.9	225.4	3.43	86.2	897.8	1259.5	1443
2	20.0	3.9	2174.4	1083.8	241.8	3.71	85.5	822.9	1265.9	1281
3	22.6	2.6	1160.3	536.9	261.5	4.27	111.8	712.9	336.5	817
4	9.5	7.3	1193.8	588.8	207.6	3.84	37.6	584.4	571.9	1005
5	7.7	6.2	817.1	395.5	209.6	4.10	26.5	482.5	308.1	573
6	22.8	3.3	446.0	187.5	270.8	4.69	74.7	362.3	8.8	66
7	2.8	5.7	879.2	432.1	200.1	3.33	41.2	364.8	473.2	690
8	-2.6	2.2	585.3	103.1	176.5	3.33	22.8	421.8	140.8	756
9	-2.5	2.8	651.3	172.4	157.2	2.93	25.1	391.3	234.9	1265
10	-6.7	2.4	567.8	169.2	163.4	2.80	31.8	334.9	201.2	462
11	-6.3	3.8	574.2	224.2	155.7	2.90	26.7	311.5	236.0	905
12	-10.3	2.8	409.7	134.4	145.1	2.38	44.4	238.6	126.6	414
13	12.7	8.5	1132.4	630.4	213.3	3.58	114.6	618.9	398.9	918
14	13.7	8.7	1094.7	785.0	225.8	3.35	157.8	507.3	429.3	900
15	22.6	3.8	688.9	560.0	273.1	2.82	175.3	286.0	227.5	493
16	24.0	2.2	1324.6	805.3	249.5	3.20	194.5	547.8	582.0	1034
17	17.7	4.5	259.8	254.6	260.6	1.89	114.2	124.4	22.5	139
18	12.0	6.1	538.7	278.6	196.1	2.60	86.6	217.3	234.1	752
19	18.2	7.3	735.1	791.9	258.4	2.22	146.3	252.1	336.3	536
20	-7.0	3.9	543.3	460.8	236.1	1.71	79.5	109.9	353.7	332
21	-8.2	6.9	416.6	416.2	176.1	1.71	55.6	124.8	236.0	340
22	-5.5	4.8	506.9	261.0	159.0	2.48	36.9	221.6	248.2	699
23	22.1	6.0	1641.9	1034.7	240.6	3.35	141.1	743.0	757.6	986
24	-0.8	4.9	645.2	255.7	169.7	1.73	155.0	219.5	270.7	1733
25	17.4	7.9	976.1	700.4	225.3	3.42	75.3	431.9	468.5	672
26	4.3	4.8	389.7	299.8	221.8	1.54	117.4	92.5	179.8	713
27	19.9	6.4	101.9	194.2	285.4	0.98	51.8	36.7	13.0	109
28	20.9	6.0	68.6	75.4	284.7	0.75	46.0	19.9	2.0	82
29	20.6	5.8	1810.8	539.1	227.8	3.31	209.2	602.9	998.8	1117
30	5.3	4.1	695.8	280.2	194.0	2.19	206.9	290.8	198.1	894
31	12.7	8.6	785.6	572.7	228.6	2.97	155.4	399.7	230.6	692
32	15.6	9.5	351.0	393.3	258.4	2.53	97.1	171.5	82.1	283
33	-32.8	12.7	152.9	215.5	156.9	0.00	21.0	0.0	121.4	39
Land	8.1		770.3			2.35	96.2	331.4	341.6	617.8
Forest*	10.6		1262.3			3.46	60.4	592.6	609.4	992.8

* forest denotes biomes 1 to 12

Table 4-3. Calibrated parameters in Sim-CYCLE equilibrium run.

Term	biome 1	2	3	4	5	6	7	8
plant parameters								
ALP	0.10	0.10	0.10	0.10	0.10	0.10	0.10	0.10
KA_0	0.50	0.50	0.50	0.52	0.52	0.52	0.52	0.54
SLA	175	165	155	165	165	145	150	130
KM_{AE}	0.34	0.35	0.34	0.34	0.34	0.31	0.31	0.34
KM_{CD}	33	33	33	30	30	30	28	30
PC_{SAT0}	15	15	15	14	14	14	14	13
QE_0	0.05	0.05	0.05	0.05	0.05	0.05	0.05	0.05
QT	2.0	2.0	2.0	2.0	2.0	2.0	2.0	2.0
$SARG_F$	0.56	0.56	0.56	0.56	0.56	0.55	0.55	0.55
$SARG_C$	0.20	0.20	0.20	0.20	0.20	0.20	0.20	0.20
$SARG_R$	0.28	0.29	0.29	0.28	0.28	0.29	0.29	0.29
$SARM_F$	1.60	1.61	1.60	1.61	1.61	1.52	1.49	1.49
$SARM_C$ (sap)	0.068	0.068	0.068	0.070	0.070	0.070	0.069	0.700
(heart)	0.0037	0.0039	0.0040	0.0040	0.0040	0.0043	0.0040	0.0046
$SARM_R$ (sap)	0.250	0.260	0.265	0.260	0.260	0.263	0.260	0.265
(heart)	0.0185	0.0190	0.0190	0.0190	0.0190	0.0193	0.0190	0.0200
SLF_F ($\times 10^{-3}$)	2.38	2.48	2.38	2.05	1.90	1.50	1.30	1.30
SLF_C ($\times 10^{-3}$)	0.070	0.070	0.070	0.069	0.071	0.071	0.072	0.072
SLF_R ($\times 10^{-3}$)	0.39	0.39	0.38	0.39	0.40	0.40	0.40	0.41
T_{OPT}	25	25	25	20	20	20	22	18
T_{MIN}	8	6	8	4	4	4	4	0
T_{MAX}	45	45	45	42	42	42	44	40
χ_1	10	10	10	10	10	10	10	10
χ_2 ($\times 10^3$)	210	210	200	200	200	195	183	170
χ_3	4.8	4.8	5.1	5.0	5.0	5.4	5.8	5.0
PT to WP_C	0.52	0.51	0.52	0.51	0.52	0.52	0.52	0.52
soil parameters								
$KM_{WA,L}$	0.21	0.20	0.21	0.20	0.20	0.20	0.20	0.20
$KM_{AE,L}$	0.23	0.20	0.23	0.22	0.22	0.20	0.22	0.22
$KM_{WA,H}$	0.11	0.11	0.11	0.11	0.11	0.11	0.11	0.10
$KM_{AE,H}$	0.10	0.10	0.10	0.10	0.10	0.10	0.10	0.08
HM	1.38	1.38	1.38	1.38	1.38	1.38	1.38	1.38
SHR_L	1.40	1.40	1.30	1.40	1.40	1.35	1.40	1.40
SHR_H	0.119	0.122	0.116	0.133	0.142	0.116	0.147	0.182

Table 4-3 (continued).

Term	biome 9	10	11	12	13	14 C_3	C_4
plant parameters							
ALP	0.10	0.10	0.10	0.10	0.10	0.15	0.10
KA_0	0.54	0.54	0.54	0.54	0.50	0.42	0.40
SLA	120	120	110	110	135	140	140
KM_{AE}	0.34	0.32	0.34	0.32	0.32	0.32	0.20
KM_{CD}	30	30	30	30	30	40	10
PC_{SAT0}	13	13	13	13	13	13	15
QE_0	0.05	0.05	0.05	0.05	0.05	0.05	0.05
QT	2.0	2.0	2.0	2.0	2.0	2.0	2.0
$SARG_F$	0.55	0.55	0.55	0.55	0.59	0.59	0.60
$SARG_C$	0.20	0.20	0.20	0.20	0.30	0.32	0.40
$SARG_R$	0.29	0.29	0.29	0.29	0.39	0.40	0.50
$SARM_F$	1.49	1.49	1.49	1.49	1.70	1.77	2.00
$SARM_C$ (sap)	0.070	0.070	0.070	0.070	0.090	0.100	0.500
(heart)	0.0046	0.0046	0.0048	0.0048	-	-	-
$SARM_R$ (sap)	0.265	0.265	0.265	0.265	0.350	0.520	0.900
(heart)	0.0200	0.0200	0.0205	0.0205	-	-	-
SLF_F ($\times 10^{-3}$)	1.30	1.30	1.30	1.50	2.30	2.10	2.90
SLF_C ($\times 10^{-3}$)	0.072	0.072	0.072	0.072	0.093	0.102	0.190
SLF_R ($\times 10^{-3}$)	0.41	0.41	0.41	0.41	0.83	1.03	2.30
T_{OPT}	18	18	18	18	22	22	30
T_{MIN}	0	0	-1	-1	0	0	8
T_{MAX}	40	40	40	40	40	40	45
χ_1	10	10	10	10	10	10	10
χ_2 ($\times 10^3$)	170	170	170	170	190	190	170
χ_3	5.0	5.2	5.0	5.2	5.0	4.5	7.0
PT to WP_C	0.50	0.49	0.50	0.49	0.45	0.30	0.10
soil parameters							
$KM_{WA,L}$	0.22	0.21	0.21	0.21	0.22	0.20	-
$KM_{AE,L}$	0.21	0.18	0.21	0.18	0.21	0.20	-
$KM_{WA,H}$	0.10	0.10	0.10	0.10	0.11	0.11	-
$KM_{AE,H}$	0.08	0.08	0.08	0.08	0.10	0.10	-
HM	1.28	1.28	1.28	1.28	1.47	1.47	-
SHR_L	1.40	1.50	1.40	1.50	1.32	1.32	-
SHR_H	0.167	0.197	0.187	0.197	0.110	0.112	-

Table 4-3 (continued).

Term	biome 15		16		17		18	
plant parameter.	C_3	C_4	C_3	C_4	C_3	C_4	C_3	C_4
ALP	0.15	0.10	0.15	0.10	0.15	0.10	0.15	0.10
KA_0	0.42	0.40	0.42	0.40	0.42	0.40	0.42	0.40
SLA	140	120	140	140	140	140	135	140
KM_{AE}	0.32	0.20	0.32	0.20	0.31	0.20	0.31	0.20
KM_{CD}	40	10	40	10	37	10	40	10
PC_{SAT0}	12	15	14	15	14	15	13	15
QE_0	0.05	0.05	0.05	0.05	0.05	0.05	0.05	0.05
QT	2.0	2.0	2.0	2.0	2.0	2.0	2.0	2.0
$SARG_F$	0.59	0.60	0.59	0.60	0.57	0.60	0.59	0.60
$SARG_C$	0.32	0.40	0.32	0.40	0.25	0.40	0.35	0.40
$SARG_R$	0.40	0.50	0.40	0.50	0.34	0.50	0.40	0.50
$SARM_F$	1.75	2.00	1.75	2.00	1.63	2.00	1.70	2.00
$SARM_C$ (sap)	0.100	0.500	0.100	0.500	0.092	0.500	0.100	0.500
(heart)	-	-	-	-	-	-	-	-
$SARM_R$ (sap)	0.450	0.900	0.450	0.900	0.450	0.900	0.570	0.900
(heart)	-	-	-	-	-	-	-	-
SLF_F ($\times 10^{-3}$)	2.30	3.10	2.50	3.10	2.10	2.80	2.50	2.80
SLF_C ($\times 10^{-3}$)	0.124	0.190	0.101	0.190	0.101	0.190	0.116	0.190
SLF_R ($\times 10^{-3}$)	1.10	2.30	0.88	2.30	0.95	2.30	1.03	2.30
T_{OPT}	22	30	23	30	22	30	20	30
T_{MIN}	0	8	3	8	0	8	0	8
T_{MAX}	45	45	45	45	45	45	45	45
χ_1	10	10	10	10	10	10	10	10
χ_2 ($\times 10^3$)	170	170	190	170	190	170	180	170
χ_3	4.5	7.0	4.5	7.0	4.7	7.0	4.5	7.0
PT to WP_C	0.13	0.10	0.13	0.10	0.18	0.10	0.15	0.10
soil parameters								
$KM_{WA,L}$	0.23	-	0.23	-	0.23	-	0.20	-
$KM_{AE,L}$	0.20	-	0.20	-	0.20	-	0.21	-
$KM_{WA,H}$	0.11	-	0.11	-	0.11	-	0.11	-
$KM_{AE,H}$	0.10	-	0.10	-	0.10	-	0.10	-
HM	1.47	-	1.47	-	1.47	-	1.47	-
SHR_L	1.27	-	1.27	-	1.27	-	1.31	-
SHR_H	0.093	-	0.093	-	0.097	-	0.120	-

Table 4-3 (continued).

Term	biome 19		20	21	22	23	24	25
plant parameters	C_3	C_4						
ALP	0.15	0.10	0.10	0.10	0.10	0.10	0.10	0.10
KA_0	0.42	0.40	0.50	0.50	0.50	0.50	0.50	0.50
SLA	140	140	140	120	130	140	140	140
KM_{AE}	0.32	0.20	0.32	0.32	0.32	0.32	0.32	0.32
KM_{CD}	40	10	40	25	25	30	30	30
PC_{SAT0}	14	15	13	12	13	13	13	13
QE_0	0.05	0.05	0.05	0.05	0.05	0.05	0.05	0.05
QT	2.0	2.0	2.0	2.0	2.0	2.0	2.0	2.0
$SARG_F$	0.59	0.60	0.57	0.57	0.57	0.57	0.57	0.57
$SARG_C$	0.35	0.40	0.31	0.30	0.30	0.30	0.30	0.30
$SARG_R$	0.43	0.50	0.39	0.38	0.36	0.38	0.38	0.38
$SARM_F$	1.70	2.00	1.61	1.55	1.53	1.67	1.62	1.67
$SARM_C$ (sap)	0.100	0.500	0.095	0.095	0.085	0.100	0.100	0.100
(heart)	-	-	-	-	-	-	-	-
$SARM_R$ (sap)	0.570	0.900	0.510	0.460	0.390	0.480	0.450	0.470
(heart)	-	-	-	-	-	-	-	-
SLF_F ($x10^{-3}$)	2.50	2.90	1.70	1.50	1.60	2.50	2.50	2.50
SLF_C ($x10^{-3}$)	0.128	0.190	0.128	0.108	0.092	0.098	0.084	0.088
SLF_R ($x10^{-3}$)	1.13	2.30	0.93	0.98	0.82	0.86	0.79	0.75
T_{OPT}	23	30	18	18	18	20	20	20
T_{MIN}	3	8	-1	-3	-2	0	0	0
T_{MAX}	45	45	40	40	40	40	40	40
χ_1	10	10	10	10	10	10	10	10
χ_2 ($x10^3$)	190	170	170	170	170	190	190	190
χ_3	4.5	7.0	4.8	5.0	5.0	5.0	5.0	4.0
PT to WP_C	0.10	0.10	0.10	0.18	0.35	0.30	0.30	0.40
soil parameters								
$KM_{WA,L}$	0.22	-	0.20	0.21	0.21	0.22	0.22	0.22
$KM_{AE,L}$	0.22	-	0.25	0.22	0.22	0.25	0.25	0.25
$KM_{WA,H}$	0.11	-	0.11	0.10	0.10	0.11	0.11	0.11
$KM_{AE,H}$	0.10	-	0.10	0.08	0.08	0.10	0.10	0.10
HM	1.47	-	1.38	1.28	1.38	1.47	1.47	1.47
SHR_L	1.27	-	1.27	1.27	1.27	1.18	1.09	1.28
SHR_H	0.097	-	0.107	0.131	0.161	0.093	0.092	0.110

Table 4-3 (continued).

Term	biome 26	27		28		29	30	31	32
plant parameters		C_3	C_4	C_3	C_4				
ALP	0.10	0.10	0.10	0.10	0.10	0.10	0.10	0.10	0.10
KA_0	0.50	0.42	0.40	0.42	0.40	0.42	0.47	0.47	0.47
SLA	130	120	120	120	120	150	150	150	145
KM_{AE}	0.32	0.31	0.20	0.31	0.20	0.37	0.34	0.36	0.34
KM_{CD}	30	30	10	30	10	30	30	30	30
PC_{SAT0}	14	14	15	14	15	15	15	15	15
QE_0	0.05	0.05	0.05	0.05	0.05	0.05	0.05	0.05	0.05
QT	2.0	2.0	2.0	2.0	2.0	2.0	2.0	2.0	2.0
$SARG_F$	0.57	0.57	0.60	0.57	0.60	0.59	0.59	0.59	0.59
$SARG_C$	0.34	0.34	0.40	0.32	0.40	0.35	0.35	0.35	0.35
$SARG_R$	0.42	0.40	0.50	0.40	0.50	0.43	0.43	0.43	0.43
$SARM_F$	1.66	1.65	2.00	1.65	2.00	1.78	1.78	1.78	1.76
$SARM_C$ (sap)	0.090	0.100	0.500	0.100	0.500	0.100	0.100	0.100	0.100
(heart)	-	-	-	-	-	-	-	-	-
$SARM_R$ (sap)	0.450	0.500	0.900	0.500	0.900	0.540	0.540	0.540	0.540
(heart)	-	-	-	-	-	-	-	-	-
SLF_F ($x10^{-3}$)	2.60	2.75	2.90	2.60	2.90	2.10	1.70	1.70	1.70
SLF_C ($x10^{-3}$)	0.099	0.108	0.190	0.108	0.190	0.108	0.099	0.138	0.128
SLF_R ($x10^{-3}$)	0.79	0.96	2.30	1.01	2.30	1.18	0.93	1.23	1.23
T_{OPT}	20	23	30	25	30	22	20	22	20
T_{MIN}	0	0	8	3	8	5	0	3	0
T_{MAX}	40	45	45	45	45	40	40	40	40
χ_1	10	10	10	10	10	10	10	10	10
χ_2 ($x10^3$)	170	160	170	160	170	200	200	200	200
χ_3	6.0	6.0	7.0	6.0	7.0	4.0	4.5	4.0	4.5
PT to WP_C	0.45	0.30	0.10	0.30	0.10	0.10	0.25	0.20	0.19
soil parameters									
$KM_{WA,L}$	0.20	0.20	-	0.20	-	0.23	0.23	0.23	0.23
$KM_{AE,L}$	0.21	0.20	-	0.20	-	0.23	0.23	0.23	0.23
$KM_{WA,H}$	0.11	0.11	-	0.11	-	0.11	0.11	0.11	0.11
$KM_{AE,H}$	0.10	0.10	-	0.10	-	0.10	0.10	0.10	0.10
HM	1.47	1.47	-	1.47	-	1.47	1.47	1.47	1.47
SHR_L	1.37	1.33	-	1.33	-	1.38	1.36	1.34	1.35
SHR_H	0.122	0.132	-	0.132	-	0.122	0.122	0.117	0.120

Table 4-4. Average equilibrium time and *NPP* in each biome, estimated by Sim-CYCLE equilibrium run.

	Estimated carbon dynamics																
	Time		*NPP*			Monthly *NPP*											
	(years)		(Mg C ha^{-1} yr^{-1})		(Pg C yr^{-1})	(Mg C ha^{-1} mon^{-1})											
Biome	Av.	SD	Av.	SD	Total	1	2	3	4	5	6	7	8	9	10	11	12
0	-	-	-	-	-	-	-	-	-	-	-	-	-	-	-	-	-
1	280	16	10.7	2.2	11.2	0.90	0.81	0.93	0.91	0.94	0.89	0.90	0.89	0.86	0.91	0.89	0.91
2	293	31	10.4	2.6	1.2	0.83	0.75	0.88	0.89	0.94	0.88	0.88	0.87	0.85	0.89	0.85	0.85
3	386	461	8.9	2.9	4.2	0.80	0.78	0.92	0.83	0.69	0.63	0.65	0.67	0.67	0.73	0.73	0.76
4	415	218	8.9	3.2	3.1	0.27	0.28	0.41	0.57	1.19	1.39	1.41	1.25	0.93	0.55	0.36	0.28
5	457	251	7.7	3.0	1.2	0.22	0.18	0.23	0.48	1.19	1.29	1.27	1.16	0.88	0.38	0.21	0.22
6	397	239	3.2	1.8	0.3	0.23	0.33	0.44	0.41	0.34	0.25	0.24	0.24	0.23	0.20	0.17	0.17
7	550	242	5.1	3.2	1.8	0.00	0.02	0.05	0.12	0.55	1.05	1.28	1.17	0.67	0.14	0.02	0.00
8	628	261	5.8	1.2	0.9	-0.01	-0.01	-0.02	-0.04	0.81	1.41	1.58	1.42	0.77	-0.03	-0.02	-0.01
9	596	196	5.2	1.6	1.8	-0.01	-0.01	-0.03	-0.04	0.64	1.29	1.45	1.28	0.64	0.00	-0.02	-0.02
10	766	209	4.6	1.4	1.0	0.00	0.00	-0.01	-0.03	0.36	1.20	1.41	1.25	0.51	-0.03	-0.01	0.00
11	890	422	4.3	1.4	1.2	-0.01	-0.01	-0.01	-0.02	0.28	1.11	1.37	1.14	0.46	-0.01	-0.01	-0.01
12	1156	398	3.1	1.0	0.5	0.00	0.00	0.00	-0.01	0.02	0.88	1.19	0.91	0.14	-0.01	0.00	0.00
13	323	178	6.2	3.0	3.2	0.28	0.28	0.37	0.50	0.67	0.72	0.78	0.76	0.66	0.51	0.35	0.30
14	487	590	5.8	2.2	2.4	0.26	0.26	0.34	0.48	0.71	0.77	0.79	0.72	0.58	0.39	0.28	0.26
15	982	917	4.4	2.6	1.8	0.40	0.36	0.40	0.37	0.36	0.32	0.32	0.36	0.37	0.38	0.37	0.41
16	611	812	6.3	2.1	4.2	0.57	0.52	0.54	0.51	0.52	0.50	0.51	0.50	0.50	0.53	0.54	0.57
17	775	821	1.9	2.0	0.7	0.11	0.11	0.15	0.18	0.23	0.22	0.21	0.19	0.16	0.14	0.11	0.10
18	749	723	4.6	2.7	0.1	0.20	0.19	0.25	0.29	0.41	0.59	0.65	0.62	0.52	0.38	0.27	0.23
19	548	698	3.3	3.0	5.7	0.25	0.23	0.27	0.28	0.31	0.29	0.30	0.31	0.29	0.28	0.25	0.25
20	1156	612	1.6	2.0	0.1	-0.01	-0.01	0.00	0.02	0.18	0.34	0.43	0.40	0.25	0.03	0.00	0.00
21	1114	594	2.1	2.4	2.0	0.02	0.02	0.04	0.06	0.17	0.43	0.55	0.46	0.22	0.05	0.02	0.02
22	973	468	3.4	1.7	0.6	0.00	0.00	0.01	0.02	0.20	0.77	1.05	0.88	0.41	0.06	0.00	0.00
23	224	198	6.3	3.3	1.0	0.52	0.48	0.55	0.55	0.57	0.54	0.54	0.53	0.50	0.51	0.49	0.51
24	617	125	2.1	1.8	0.2	0.02	0.02	0.02	0.07	0.29	0.42	0.47	0.45	0.31	0.04	0.00	0.01
25	285	149	6.6	4.0	0.7	0.48	0.45	0.52	0.54	0.61	0.62	0.65	0.65	0.60	0.56	0.48	0.47
26	413	279	1.8	2.4	0.4	0.21	0.17	0.15	0.12	0.12	0.10	0.11	0.13	0.15	0.15	0.16	0.20
27	588	769	1.0	1.3	1.1	0.06	0.06	0.08	0.10	0.11	0.10	0.09	0.09	0.09	0.08	0.06	0.05
28	582	773	0.6	0.6	0.3	0.04	0.04	0.05	0.06	0.07	0.06	0.06	0.07	0.06	0.05	0.04	0.03
29	156	42	7.0	2.9	1.4	0.48	0.46	0.54	0.58	0.61	0.59	0.66	0.68	0.68	0.69	0.53	0.48
30	356	155	3.6	1.5	1.1	0.02	0.02	0.03	0.18	0.44	0.58	0.69	0.72	0.60	0.25	0.03	0.02
31	362	313	4.6	3.5	6.1	0.27	0.26	0.30	0.33	0.42	0.47	0.54	0.57	0.52	0.40	0.28	0.27
32	540	433	2.5	2.8	0.4	0.15	0.15	0.17	0.18	0.22	0.26	0.29	0.30	0.27	0.21	0.17	0.16
33	-	-	0.0	0.0	0.0	0.00	0.00	0.00	0.00	0.00	0.00	0.00	0.00	0.00	0.00	0.00	0.00
Land			4.2		61.798	0.24	0.23	0.27	0.29	0.40	0.50	0.55	0.52	0.40	0.29	0.24	0.24

Table 4-5. Estimated properties of carbon dynamics and production efficiencies.

	Carbon dynamics												Efficiency	
	LAI		Plant C			Soil C			*NPP/ GPP*	*ARM/ AR*	Plant time	Soil time	*RUE*	*WUE*
	(ha ha^{-1})		(Mg C ha^{-1})		(Pg C)	(Mg C ha^{-1})		(Pg C)			(years)		(g C MJ^{-1})	(g C kg H_2O^{-1})
No.	Av.	SD	Av.	SD	Total	Av.	SD	Total	Av.	Av.	Av.	Av.	Av.	Av.
0	-	-	-	-	-	-	-	-	-	-	-	-	-	-
1	4.8	0.6	212.6	47.4	222.4	93.7	22.4	98.0	45.4	57.8	19.8	8.7	0.81	1.20
2	4.7	0.8	198.3	54.5	23.5	122.7	47.3	14.5	46.6	53.2	19.1	11.8	0.72	1.26
3	3.8	0.9	131.4	59.2	62.3	98.5	28.7	46.7	45.3	55.9	14.8	11.1	0.54	1.25
4	4.5	1.1	145.1	77.1	51.3	211.0	98.8	74.7	53.3	46.1	16.3	23.7	0.60	1.52
5	5.1	1.2	137.8	65.9	20.6	218.3	92.1	32.6	53.4	45.2	17.9	28.3	0.48	1.60
6	3.0	1.2	56.3	35.3	5.1	98.6	51.2	9.0	36.3	65.5	17.3	30.4	0.18	0.90
7	4.2	1.9	95.7	66.1	33.4	193.1	97.5	67.4	51.9	38.3	18.9	38.1	0.39	1.39
8	4.4	0.4	107.9	24.9	17.1	280.7	82.2	44.4	55.0	30.3	18.5	48.1	0.45	1.38
9	3.8	1.0	91.6	30.3	31.4	237.2	77.9	81.2	54.5	29.3	17.7	45.9	0.45	1.32
10	3.6	0.9	79.3	26.0	16.7	279.6	80.7	58.8	54.8	27.4	17.1	60.4	0.43	1.38
11	3.3	0.8	72.3	25.8	19.8	298.1	119.0	81.5	54.6	25.0	16.9	69.5	0.38	1.38
12	2.4	0.7	48.3	16.4	7.8	308.4	114.5	49.6	54.3	21.6	15.6	99.8	0.33	1.30
13	3.3	1.3	71.2	38.2	36.7	121.6	51.5	62.7	41.8	41.4	11.5	19.7	0.44	1.00
14	3.1	1.2	15.2	9.2	6.2	128.3	92.7	52.3	38.4	38.3	2.6	22.0	0.45	1.15
15	2.1	1.3	7.5	5.8	3.0	60.2	33.6	24.0	33.6	41.1	1.7	13.6	0.41	1.55
16	3.3	1.2	12.2	5.9	8.2	72.9	25.0	49.2	32.3	44.5	1.9	11.6	0.51	1.15
17	1.0	1.0	5.1	7.0	1.8	53.6	63.0	19.3	41.4	37.7	2.6	28.0	0.26	1.54
18	2.4	1.4	10.7	9.7	0.2	127.0	79.2	1.9	41.5	28.7	2.3	27.7	0.45	2.11
19	1.8	1.6	6.0	6.6	10.4	55.6	41.9	96.2	34.3	40.8	1.8	16.8	0.38	1.32
20	1.4	1.6	6.3	7.7	0.5	238.9	271.1	20.2	47.2	19.9	3.8	145.7	0.25	1.49
21	1.6	1.6	11.4	13.6	11.2	231.3	226.3	228.1	48.2	21.6	5.5	111.4	0.31	1.66
22	2.7	1.1	31.9	17.0	5.5	276.3	124.7	47.9	50.1	19.4	9.4	81.5	0.35	1.53
23	3.3	1.6	50.9	28.4	8.0	79.5	44.6	12.5	36.9	53.6	8.1	12.6	0.48	0.85
24	1.4	1.1	17.6	16.1	1.7	115.0	89.1	11.1	44.9	28.9	8.4	54.7	0.31	0.96
25	3.2	1.7	75.0	47.8	7.5	117.5	76.5	11.8	39.6	49.7	11.3	17.7	0.50	1.54
26	1.0	1.3	17.7	25.2	3.5	61.1	77.2	12.2	44.3	28.7	10.0	34.6	0.30	1.91
27	0.5	0.6	1.7	2.9	1.8	15.4	20.3	17.0	36.6	38.5	1.7	16.0	0.25	2.62
28	0.3	0.3	0.9	0.7	0.4	10.2	12.0	5.3	37.1	36.7	1.3	15.9	0.22	3.22
29	3.8	2.0	22.7	16.8	4.5	62.7	19.8	12.4	36.4	46.1	3.3	9.0	0.54	1.16
30	1.3	0.9	3.8	12.3	1.1	86.2	39.0	25.5	45.8	16.2	1.1	23.9	0.42	1.24
31	2.7	2.4	15.9	21.6	21.0	92.1	48.4	121.8	39.1	40.0	3.4	20.0	0.40	1.15
32	1.6	1.8	8.1	14.5	1.3	87.9	72.1	13.8	38.5	40.0	3.2	34.6	0.26	1.48
33	0.0	0.0	0.0	0.0	0.0	0.0	0.0	0.0	-	-	-	-	-	-

Table 4-6. Zonal land area, hydrology, radiation, and carbon dynamics, estimated by Sim-CYCLE equilibrium run.

				Hydrology		Radiation		GPP	NPP						TNE	Mass				Efficiency	
		Area	(Forest)	PR	AET	Abs.R.	PAR	Total	Total	C_3	C_4		Forest			LAI	Plant	Soil C	Forest		WUE	RUE
Lat. zone	Lnad cells	(10^6 km^{-1})		(mm yr^{-1})		(GJ m^{-2} yr^{-1})	(μ mol photon m^{-2} s^{-1})	(Pg C yr^{-1})				(%)		(%)	(Pg C yr^{-1})	(-)	(Pg C)	(Pg C)	(Pg C)	(%)	(g C kg H_2O^{-1})	(g C MJ^{-1})
N90- N80	896	0.4	0.0	82	35	0.00	377	0.0	0.0	0.0	0.0	-	0.0	-	0.0	0.0	0.0	0.0	0.0	0.0	-	-
N80- N70	4357	3.6	0.1	179	87	0.50	489	0.4	0.2	0.2	0.0	0.0	0.0	6.9	0.1	0.4	1.3	36.8	2.2	5.8	1.50	0.229
N70- N60	10213	13.3	6.7	454	274	2.11	631	7.6	4.0	4.0	0.0	0.0	2.7	67.4	2.1	2.4	53.1	333.8	228.5	59.0	1.33	0.317
N60- N50	8183	14.5	6.8	668	400	2.58	847	12.0	6.1	6.1	0.0	0.0	3.5	57.5	3.3	2.8	73.0	290.5	232.6	64.0	1.35	0.365
N50- N40	7297	15.9	3.2	546	388	2.34	1156	11.2	5.5	5.5	0.0	0.3	2.3	42.0	3.1	2.0	50.4	182.2	113.1	48.6	1.31	0.327
N40- N30	6145	15.5	1.3	560	368	2.44	1427	10.8	4.8	4.4	0.3	6.6	1.0	20.1	2.0	1.7	35.3	151.6	42.2	22.6	1.28	0.279
N30- N20	5462	15.3	2.0	601	330	2.03	1601	12.7	5.2	3.9	1.3	24.2	2.1	40.3	1.3	1.8	50.6	81.4	68.9	52.2	1.33	0.372
N20- N10	3810	11.3	1.9	827	484	2.76	1525	16.1	6.0	4.0	2.1	34.2	2.2	35.8	1.2	2.6	53.2	59.6	58.5	51.8	1.33	0.427
N10- N0	3292	10.1	4.0	2025	856	3.43	1127	23.8	9.1	6.1	3.0	33.0	4.5	49.1	0.7	4.5	103.6	87.2	125.7	65.9	1.24	0.583
S0- S10	3349	10.3	5.9	2015	885	3.30	1074	23.0	9.3	7.5	1.8	19.3	6.1	65.4	0.6	4.4	130.3	90.1	170.2	77.3	1.19	0.608
S10- S20	3167	9.4	3.7	1046	722	3.63	1400	16.4	6.4	4.1	2.3	35.7	3.0	47.5	1.1	3.4	58.8	83.8	85.0	59.6	1.17	0.412
S20- S30	3345	9.4	1.0	567	436	2.55	1587	8.9	3.3	1.8	1.6	47.5	0.6	18.8	0.7	1.9	19.8	53.5	22.7	30.9	1.16	0.312
S30- S40	1647	4.2	0.4	433	392	2.82	1457	3.2	1.3	1.1	0.2	16.6	0.2	16.6	0.3	1.9	9.4	34.8	10.3	23.3	1.11	0.241
S40- S50	463	1.0	0.2	941	253	3.10	1072	1.2	0.6	0.6	0.0	0.7	0.2	33.0	0.3	3.2	6.5	15.9	7.9	35.3	3.17	0.413
S50- S60	115	0.2	0.1	1133	120	1.85	789	0.1	0.1	0.1	0.0	0.0	0.0	56.6	0.1	2.6	0.8	2.4	1.8	57.8	6.31	0.417
S60- S70	1460	1.7	0.0	342	41	0.00	583	0.0	0.0	0.0	0.0	-	0.0	-	0.0	0.0	0.0	0.0	0.0	-	-	-
S70- S80	9924	7.6	0.0	131	16	0.00	505	0.0	0.0	0.0	0.0	-	0.0	-	0.0	0.0	0.0	0.0	0.0	-	-	-
S80- S90	13580	3.5	0.0	47	6	0.00	372	0.0	0.0	0.0	0.0	-	0.0	-	0.0	0.0	0.0	0.0	0.0	-	-	-
N.Hemisph.	49655	100.0	26.0					94.5	40.8	34.2	6.6	16.3	18.2	44.6	13.8	2.33	420.5	1223.2	871.7	53.0		
S.Hemisph.	37050	47.4	11.3					52.9	21.0	15.1	5.9	28.0	10.2	48.5	3.0	2.27	225.6	280.5	297.9	58.9		
GLOBE	86705	147.4	37.3	770	428	2.35	1146	147.5	61.8	49.3	12.5	20.2	28.4	45.9	16.8	2.31	646.1	1503.7	1169.6	54.4	1.26	0.396

*TNE: Total Net Exchange: summation of the abosolute value of monthly NEP, indicating seasonal amplitude.

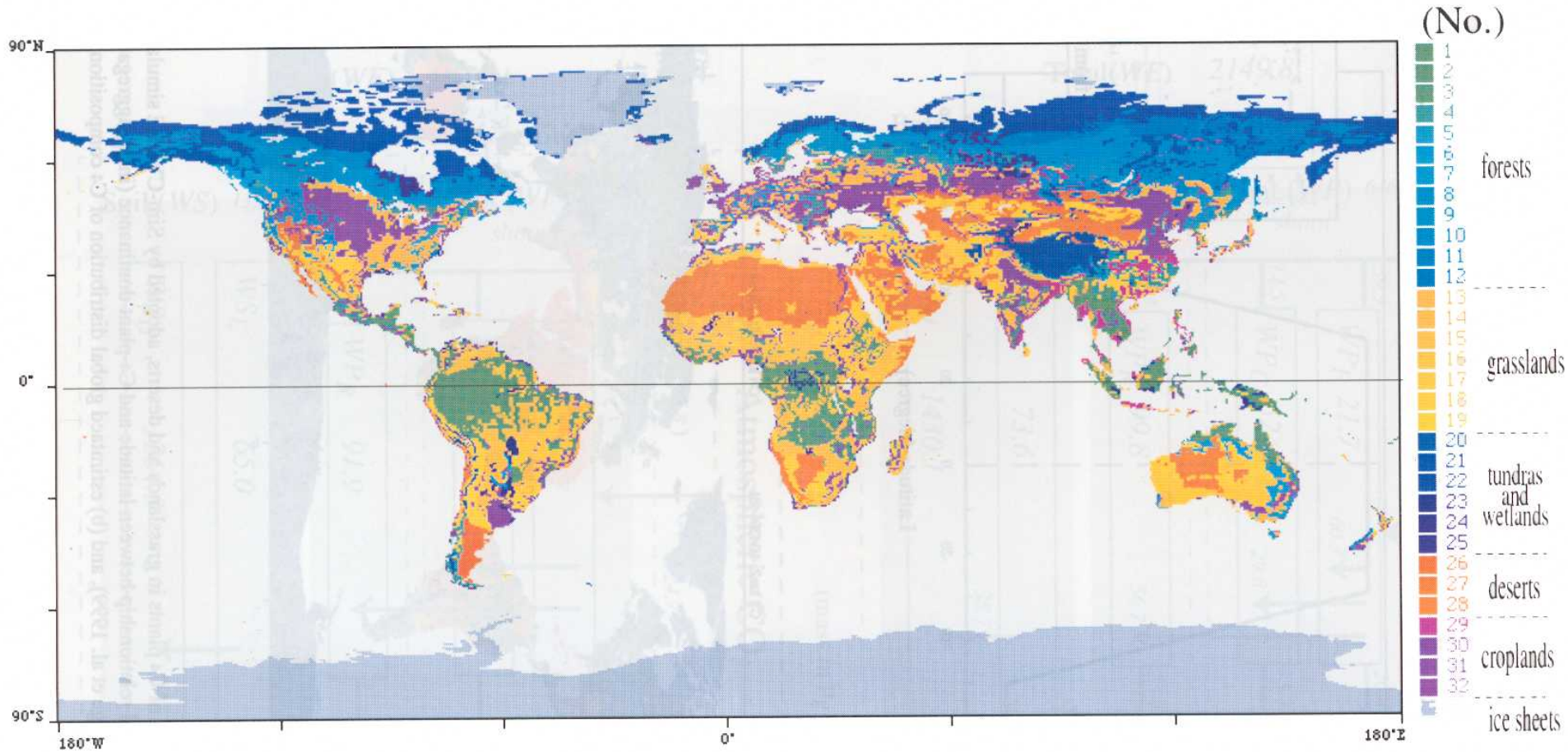

Fig. 4-1. Biome distribution (33 types) with a spatial resolution of 0.5° x 0.5° longitude-latitude, used by Sim-CYCLE equilibrium run. Original dataset was derived from Olson et al. (1983). See Table 4-1 for biome classification.

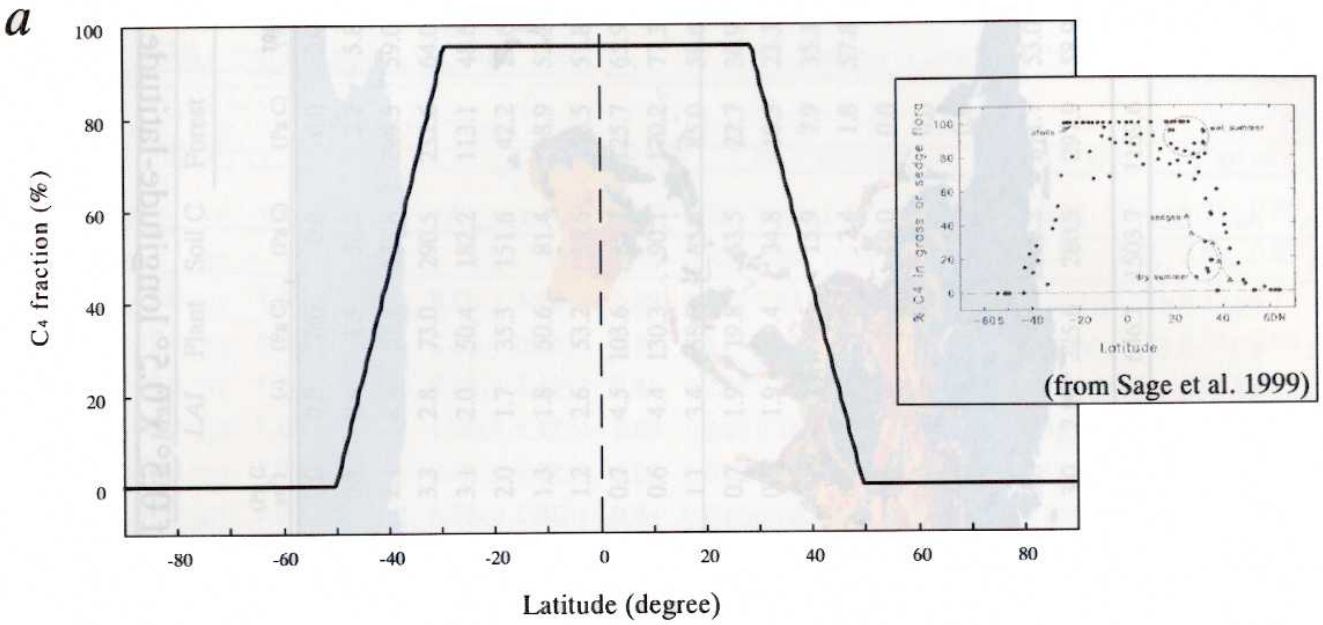

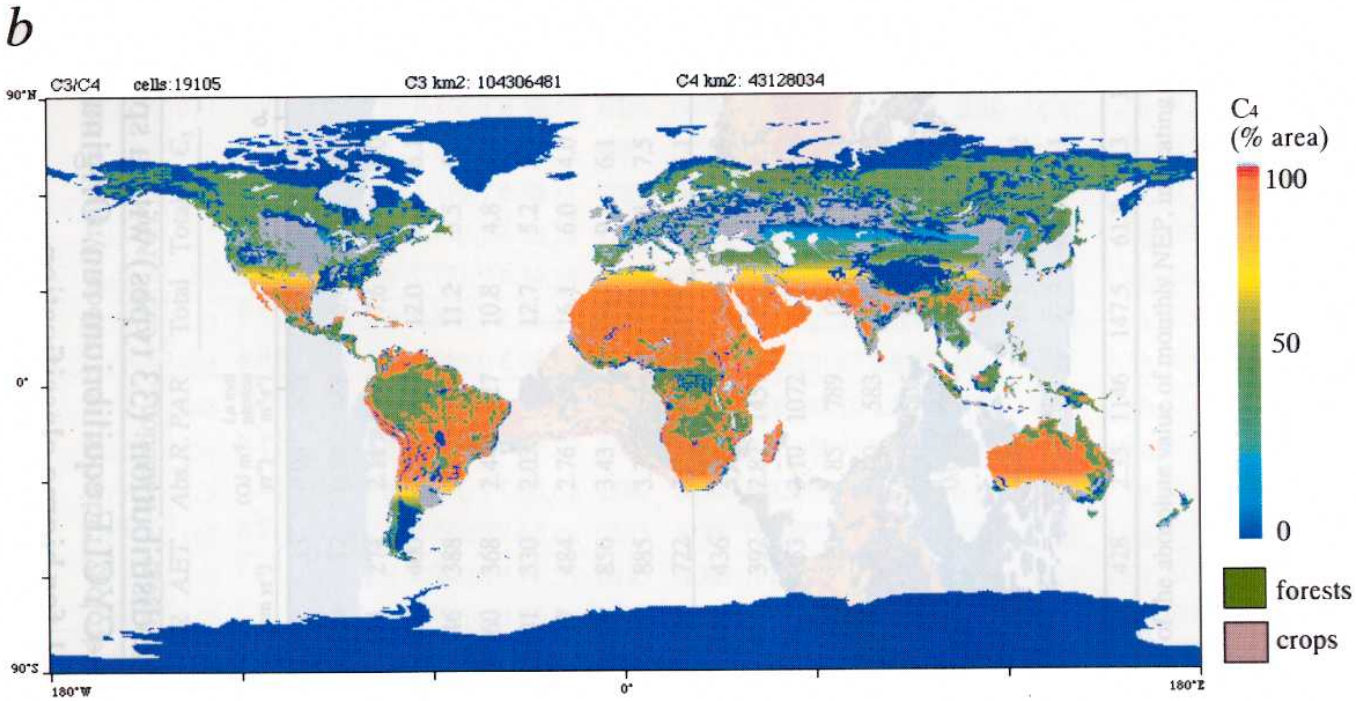

Fig.4-2. Distribution of C4 plants in grasslands and deserts, adopted by Sim-CYCLE simulations. (a) An empirical relationship between latitude and C4-plant dominance (inset, aggregation of field data by Sage et al. 1999), and (b) estimtaed global distribution of C4 composition.

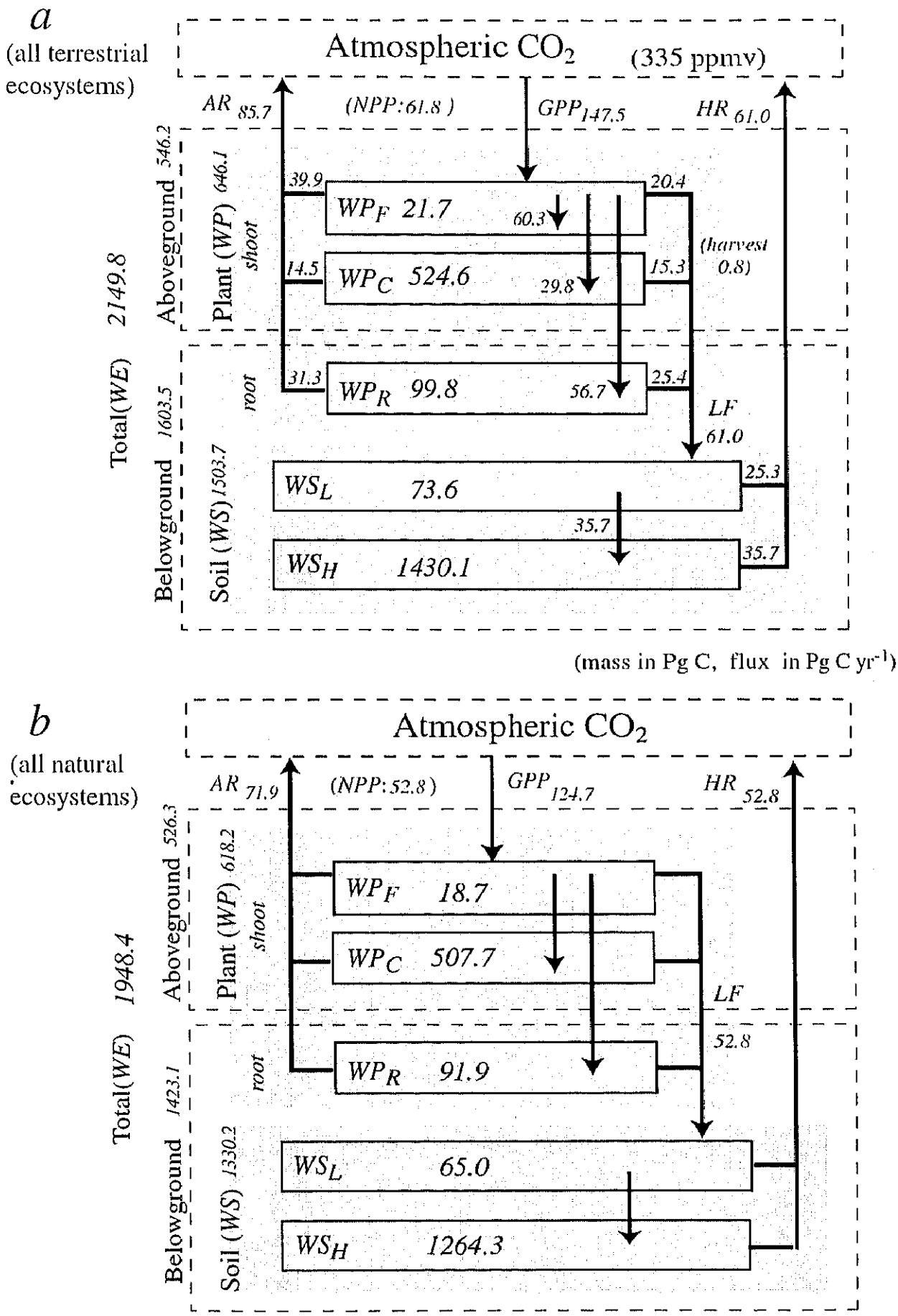

Fig. 4-3. Biospheric carbon dynamics estimated by Sim-CYCLE equilibrium run, for (a) all biomes, and (b) natural biomes (i.e. biome types 1 to 28).

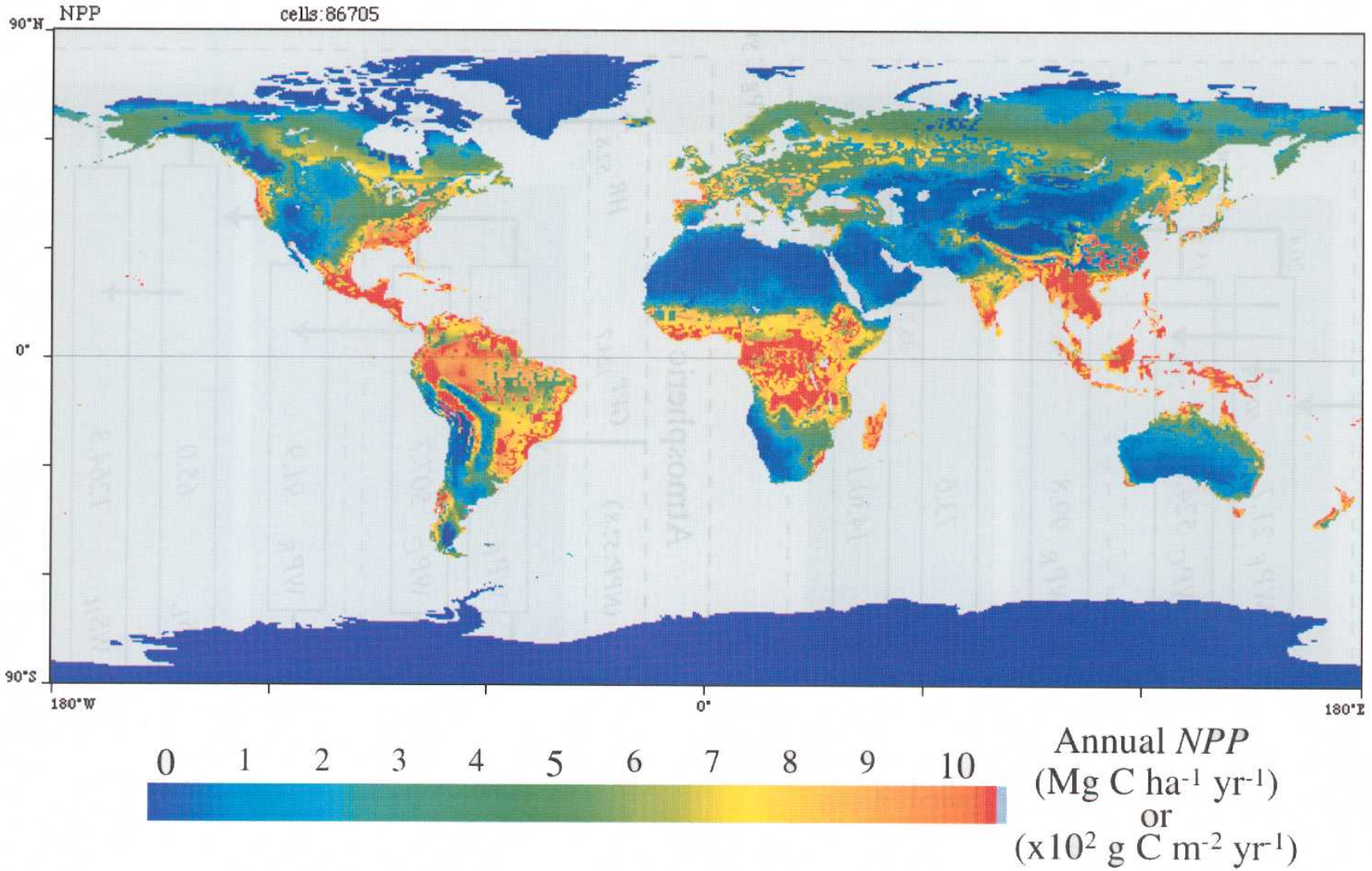

Fig. 4-4. Annual *NPP* distribution estimated by Sim-CYCLE equilibrium run.

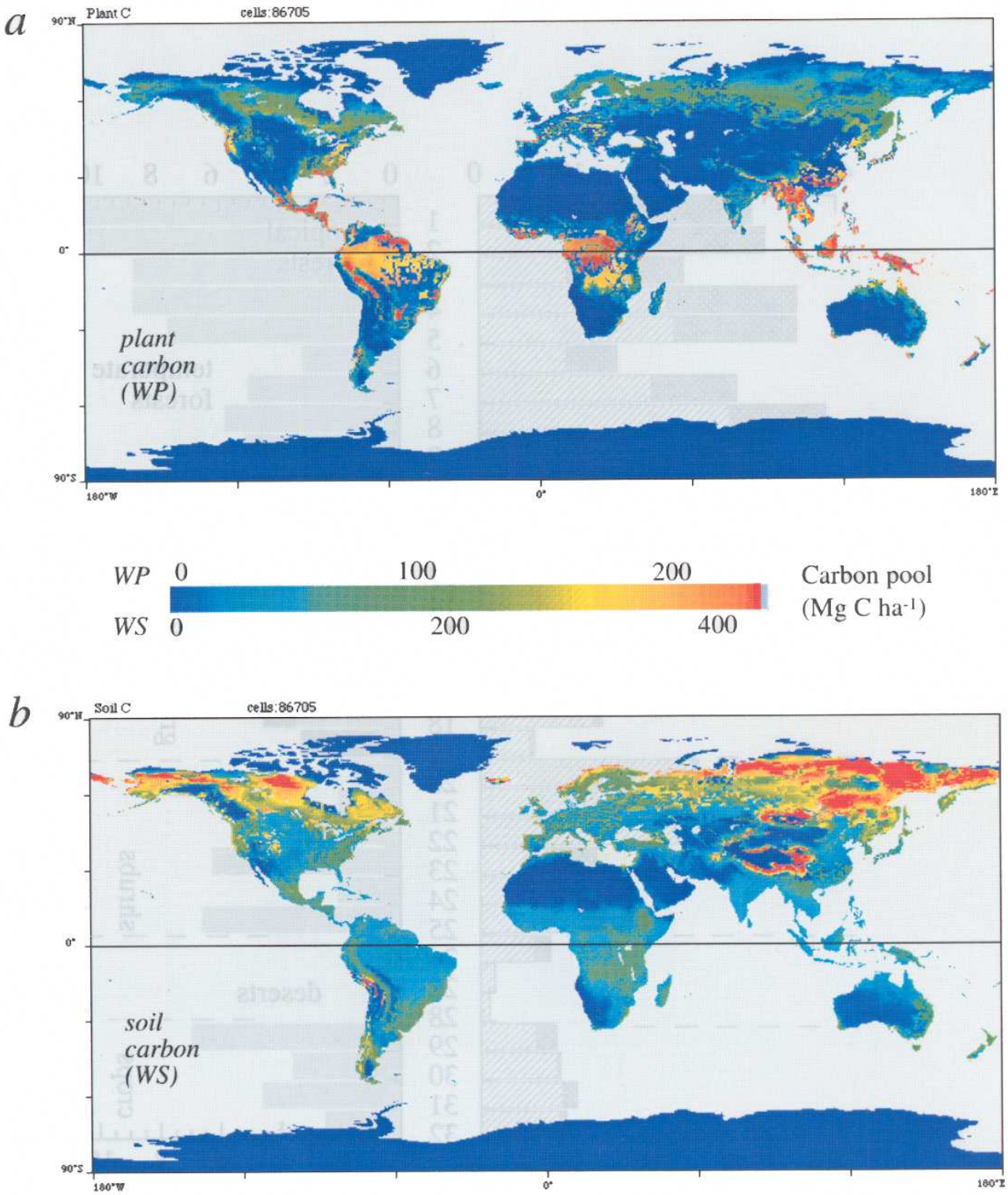

Fig. 4-5. Distribution map showing carbon storage, in (a) plant biomass and (b) soil organic matter, estimated by Sim-CYCLE equilibrium run.

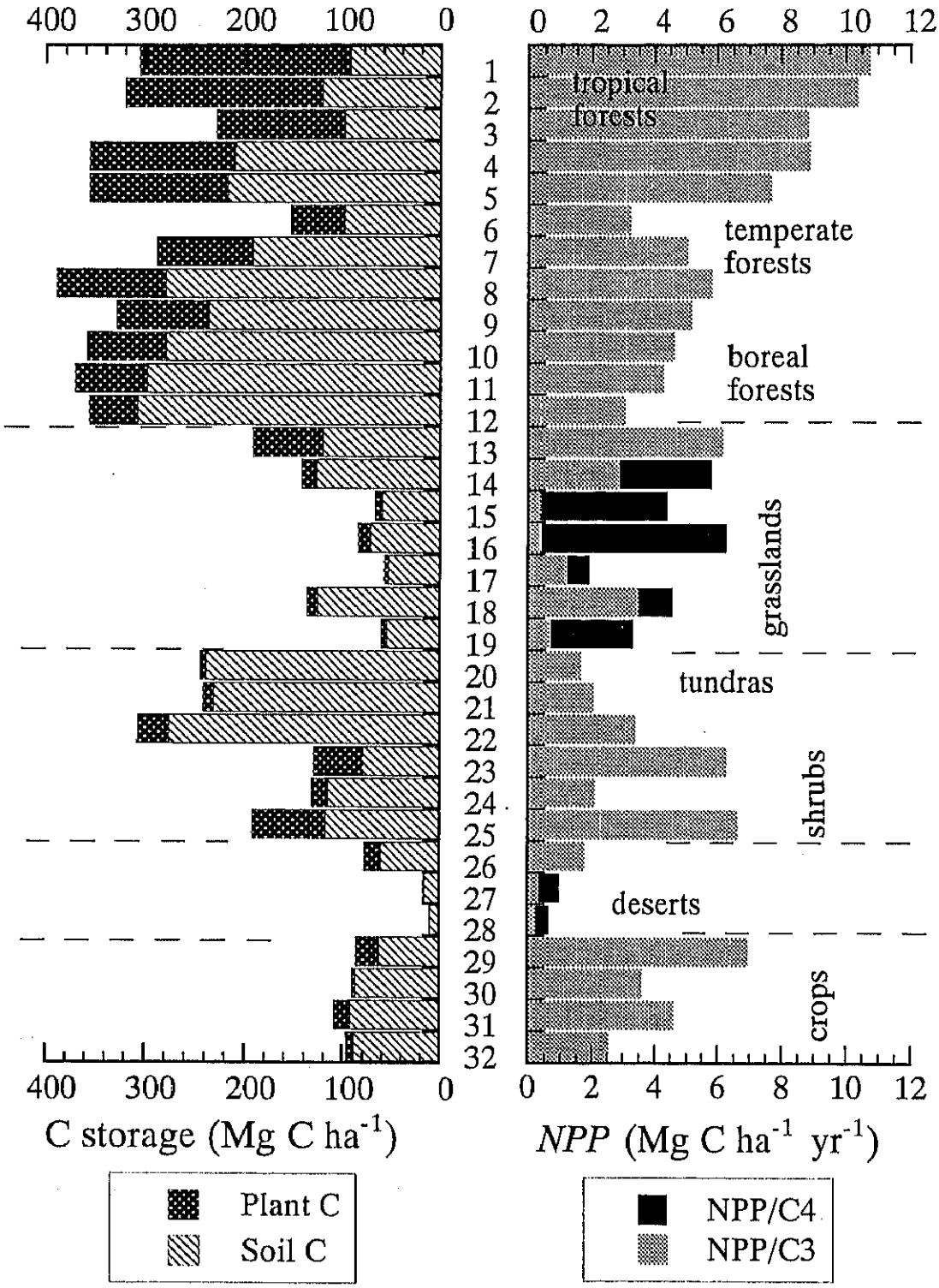

Fig. 4-6. Average carbon storage and annual *NPP* for each biome type, estimated by Sim-CYCLE equilibrium run.

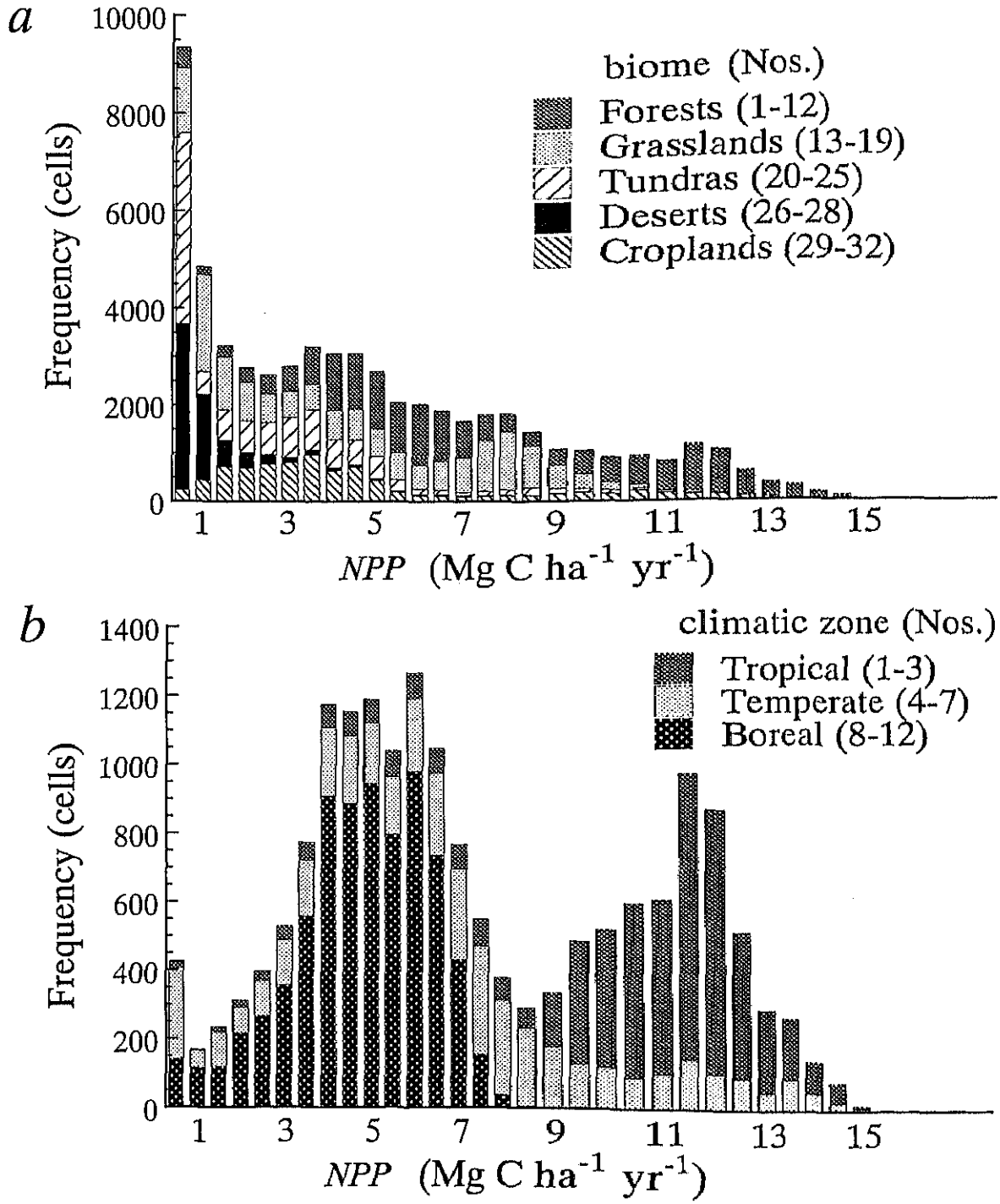

Fig. 4-7. Frequency distribution of annual *NPP*, separated by (a) aggregated biomes, and (b) climatic forest zones.

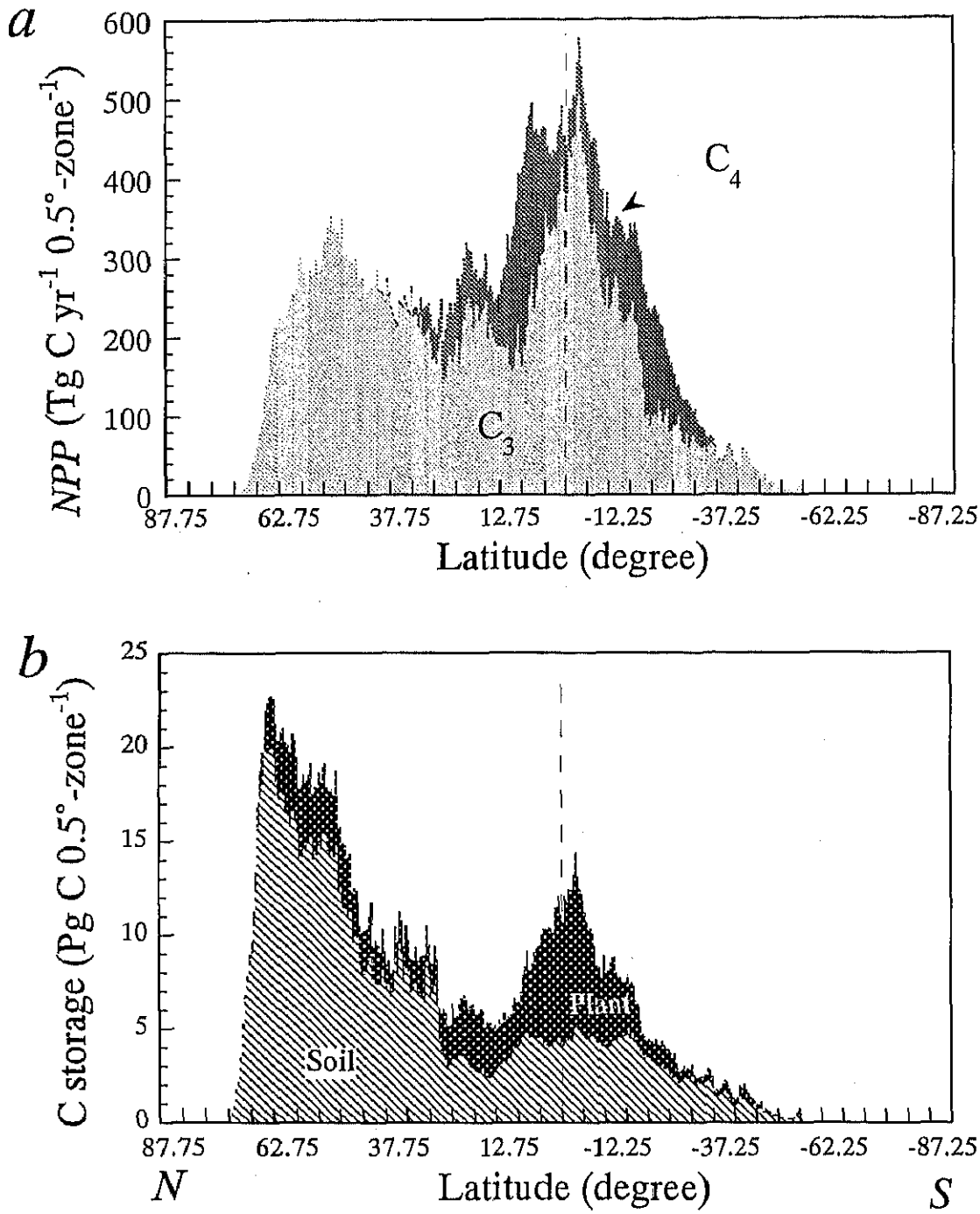

Fig. 4-8. Latitudinal distribution of (a) annual *NPP* and (b) carbon storage, estimated by Sim-CYCLE equilibrium run.

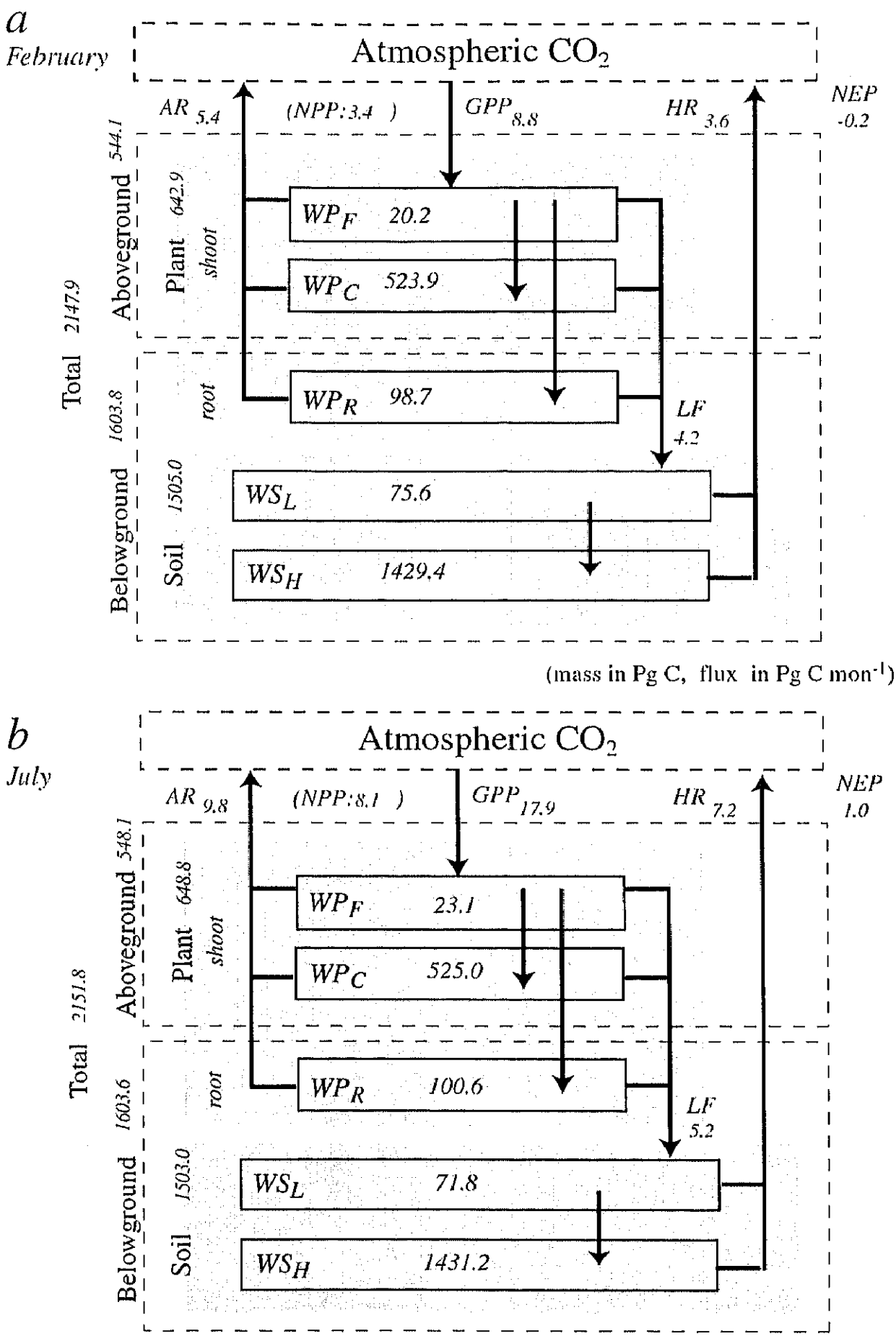

Fig. 4-9. Monthly biospheric carbon dynamics estimated by Sim-CYCLE equilibrium run, in (a) January, and (b) July.

Monthly *GPP* map

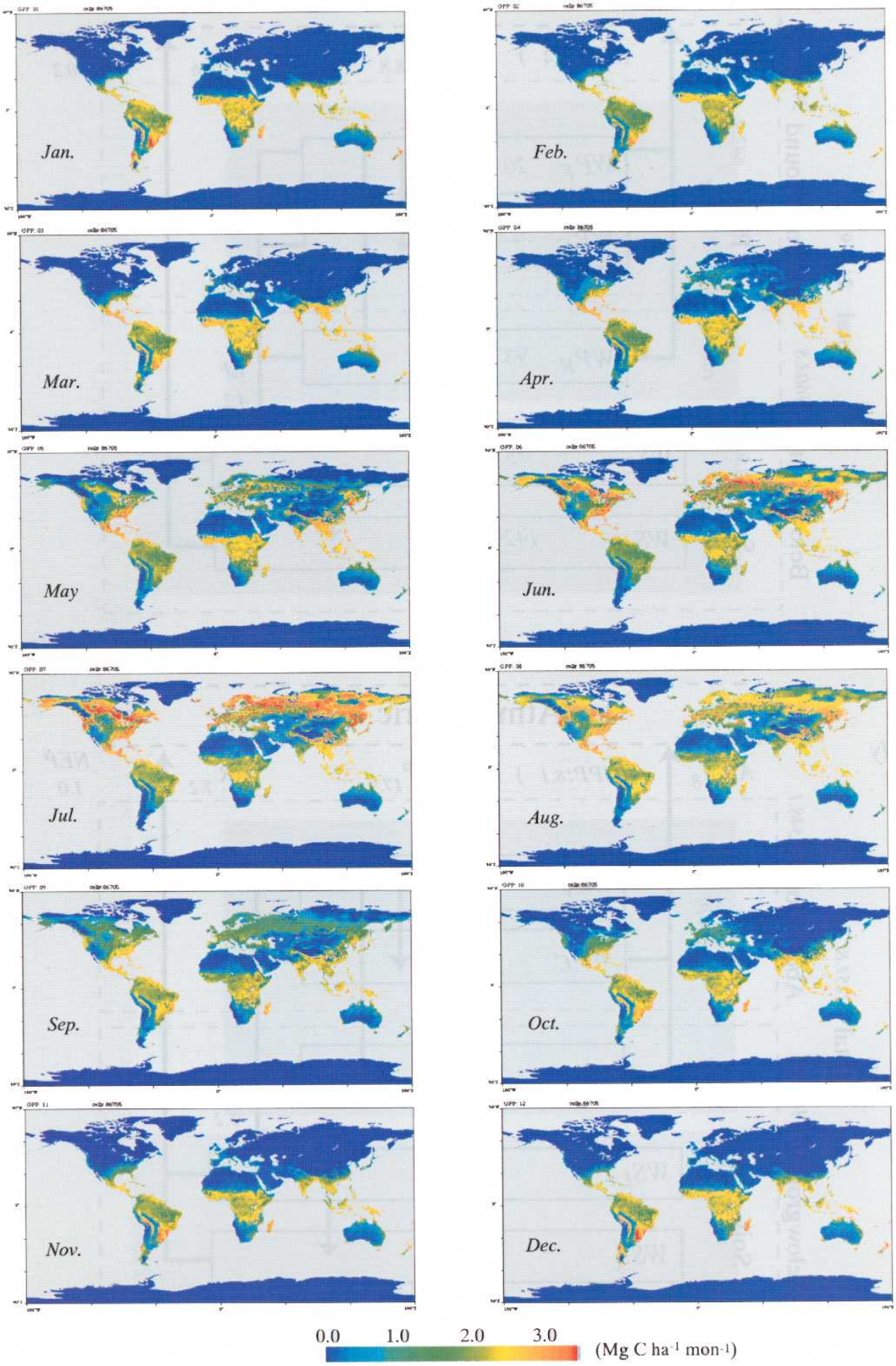

Fig. 4-10. Monthly *GPP* distribution estimated by Sim-CYCLE equilibrium run.

Monthly *NPP* map

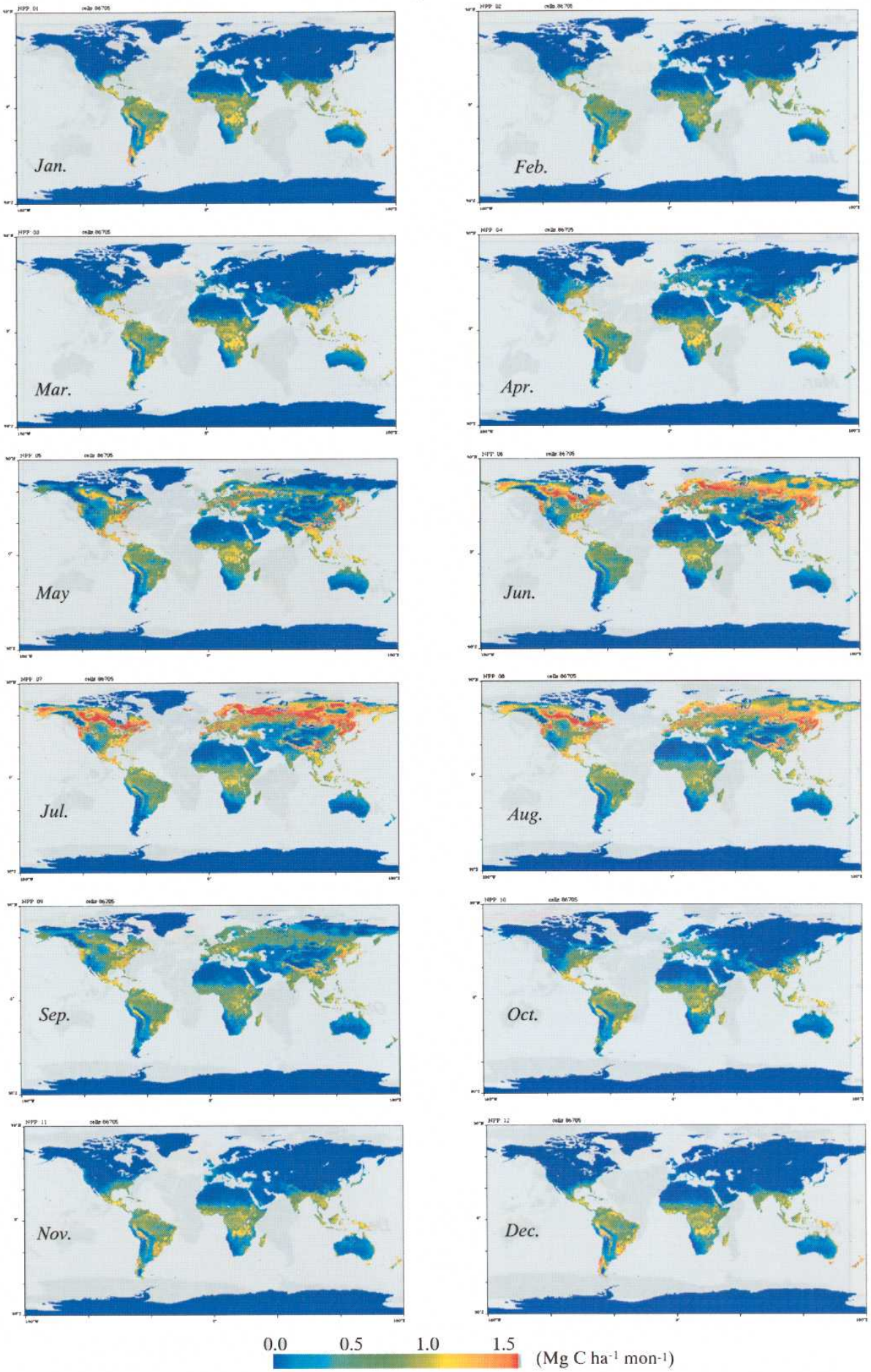

Fig. 4-11. Monthly *NPP* distribution estimated by Sim-CYCLE equilibrium run.

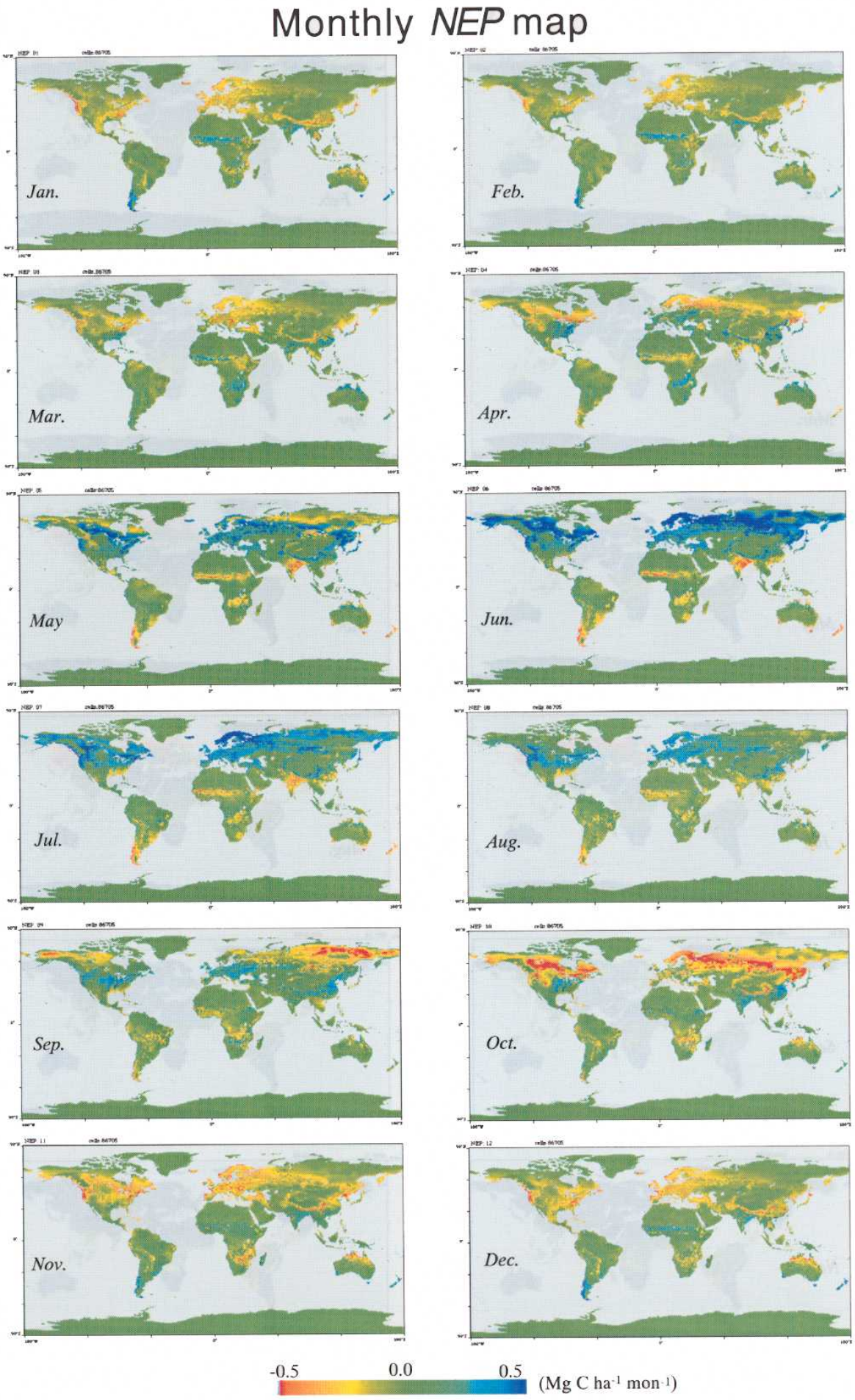

Fig. 4-12. Monthly *NEP* distribution estimated by Sim-CYCLE equilibrium run.

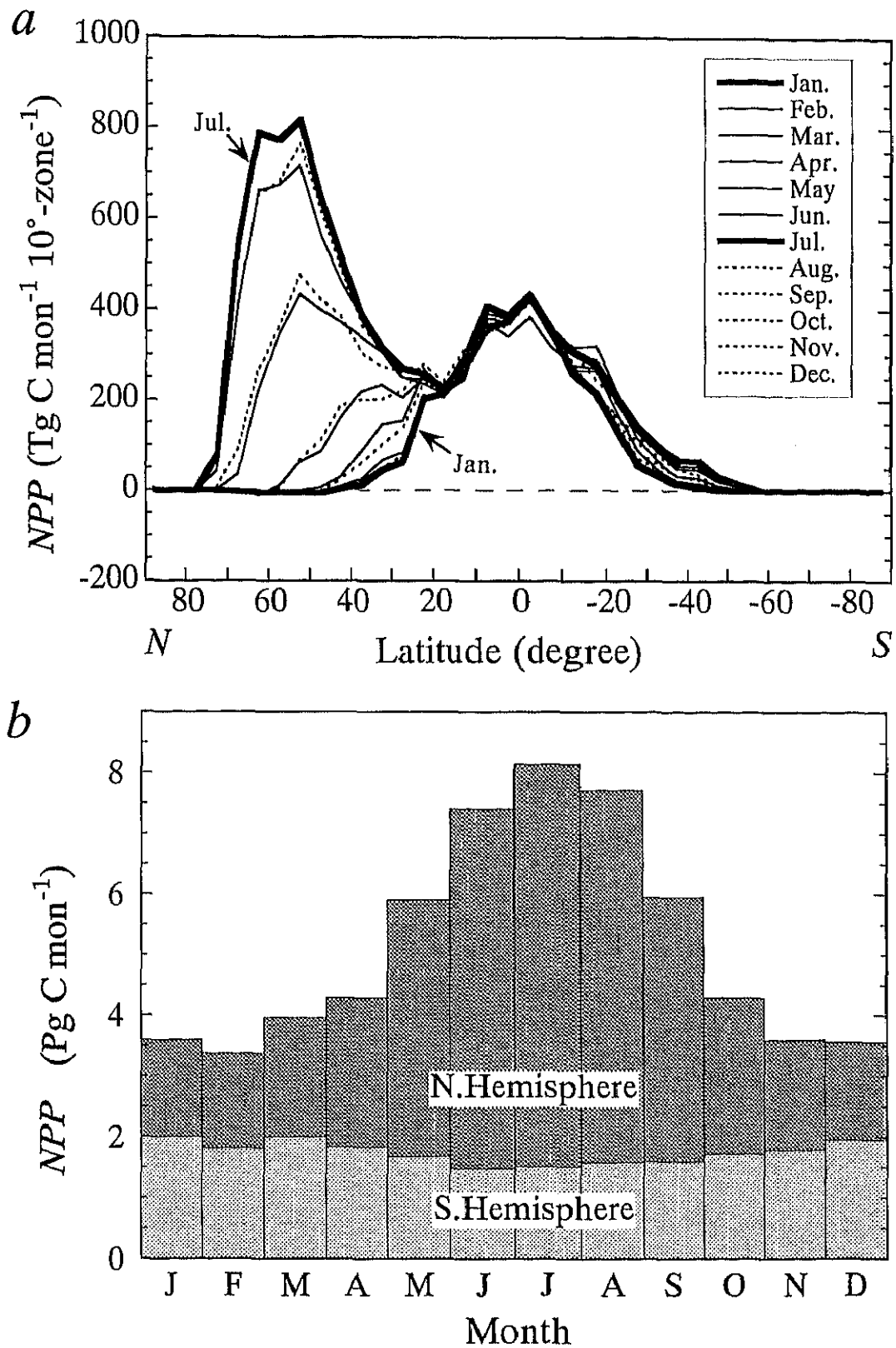

Fig. 4-13. Monthly NPP estimated by Sim-CYCLE equilibrium run. (a) Monthly *NPP* along latitudes, and (b) monthly *NPP* in the Northern and Southern Hemispheres.

Monthly *LAI* map

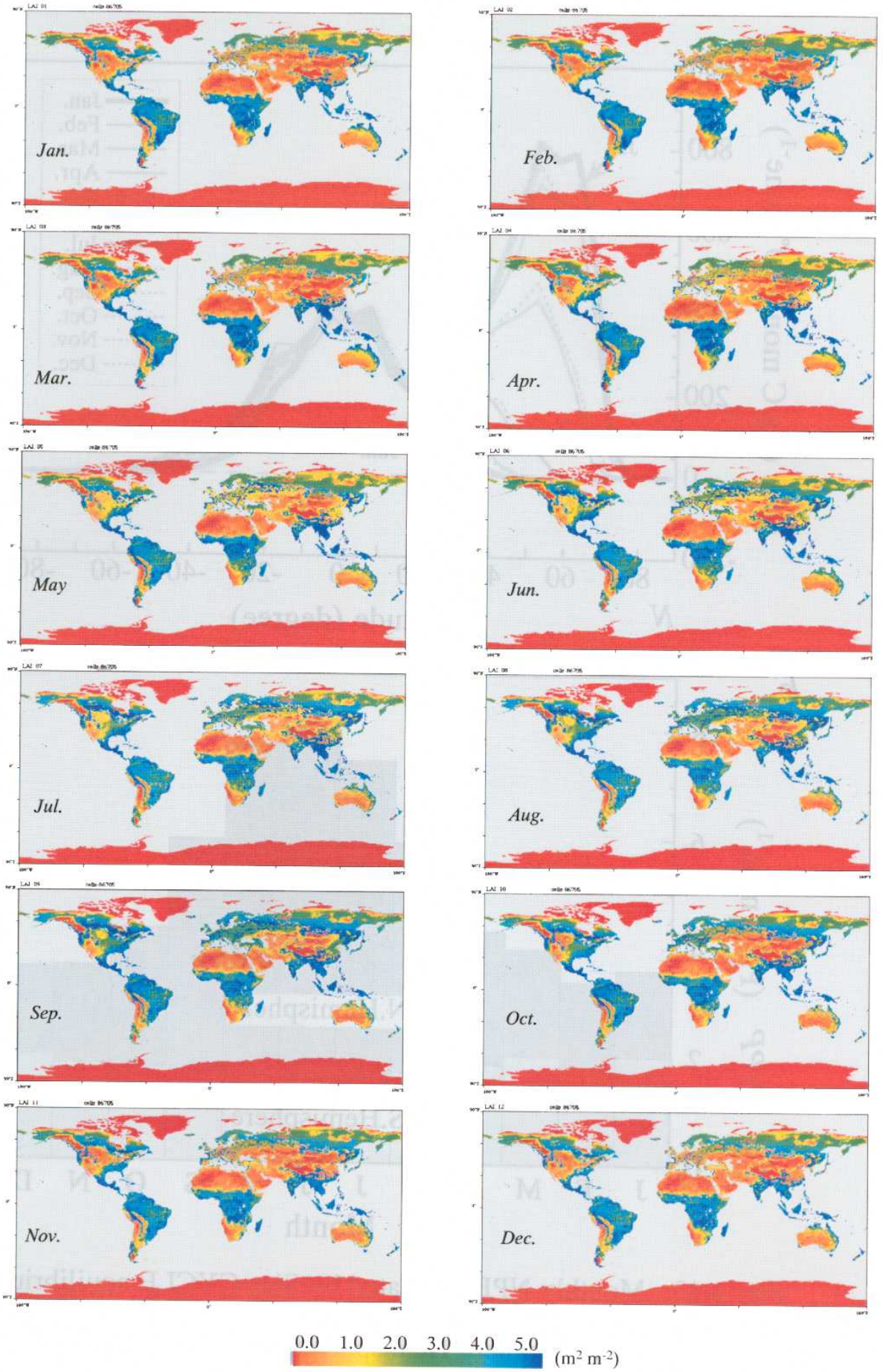

Fig. 4-14. Monthly *LAI* distribution estimated by Sim-CYCLE equilibrium run.

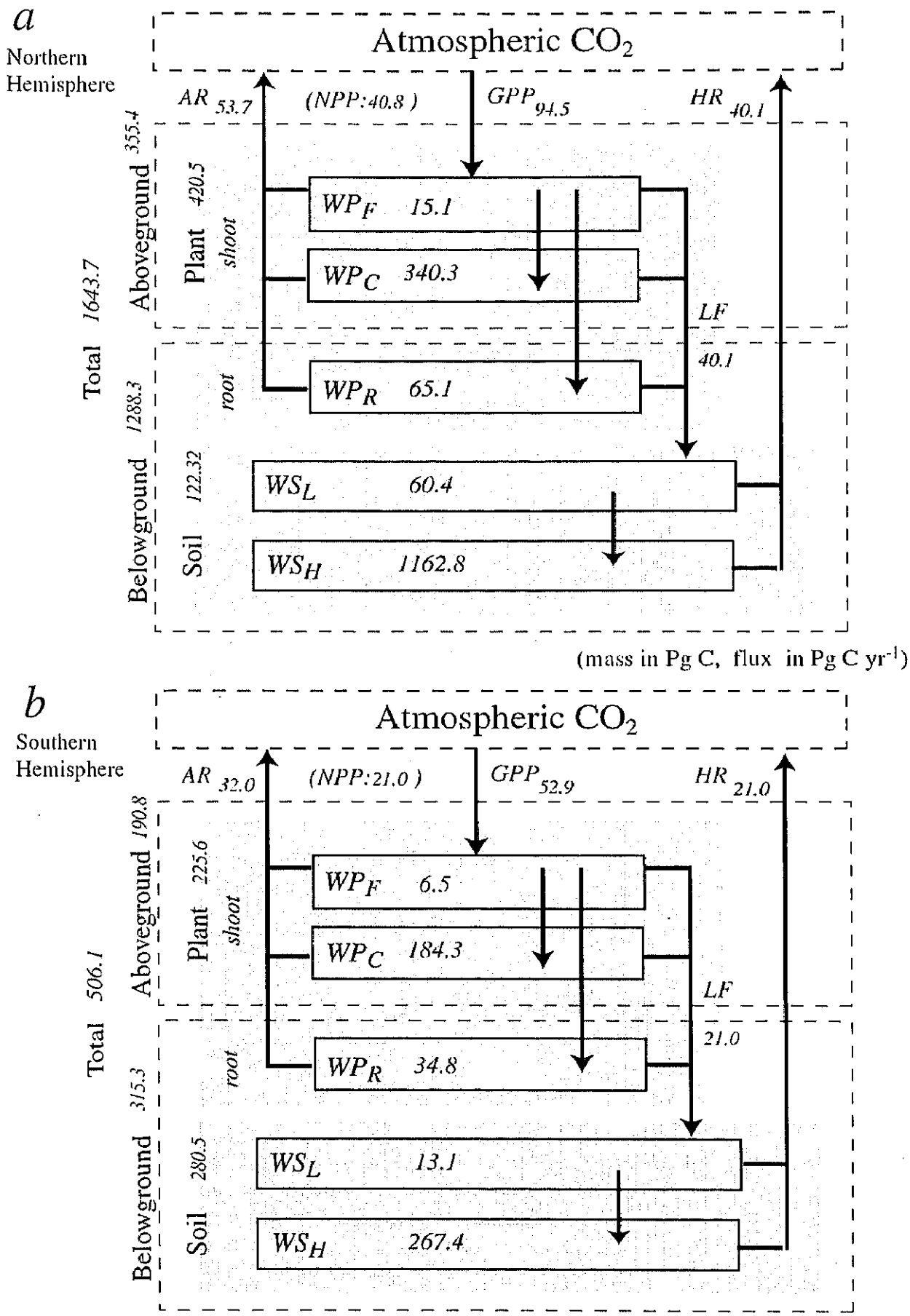

Fig. 4-15. Biospheric carbon dynamics estimated by Sim-CYCLE equilibrium run, for (a) the Northern Hemisphere, and (b) the Southern Hemisphere.

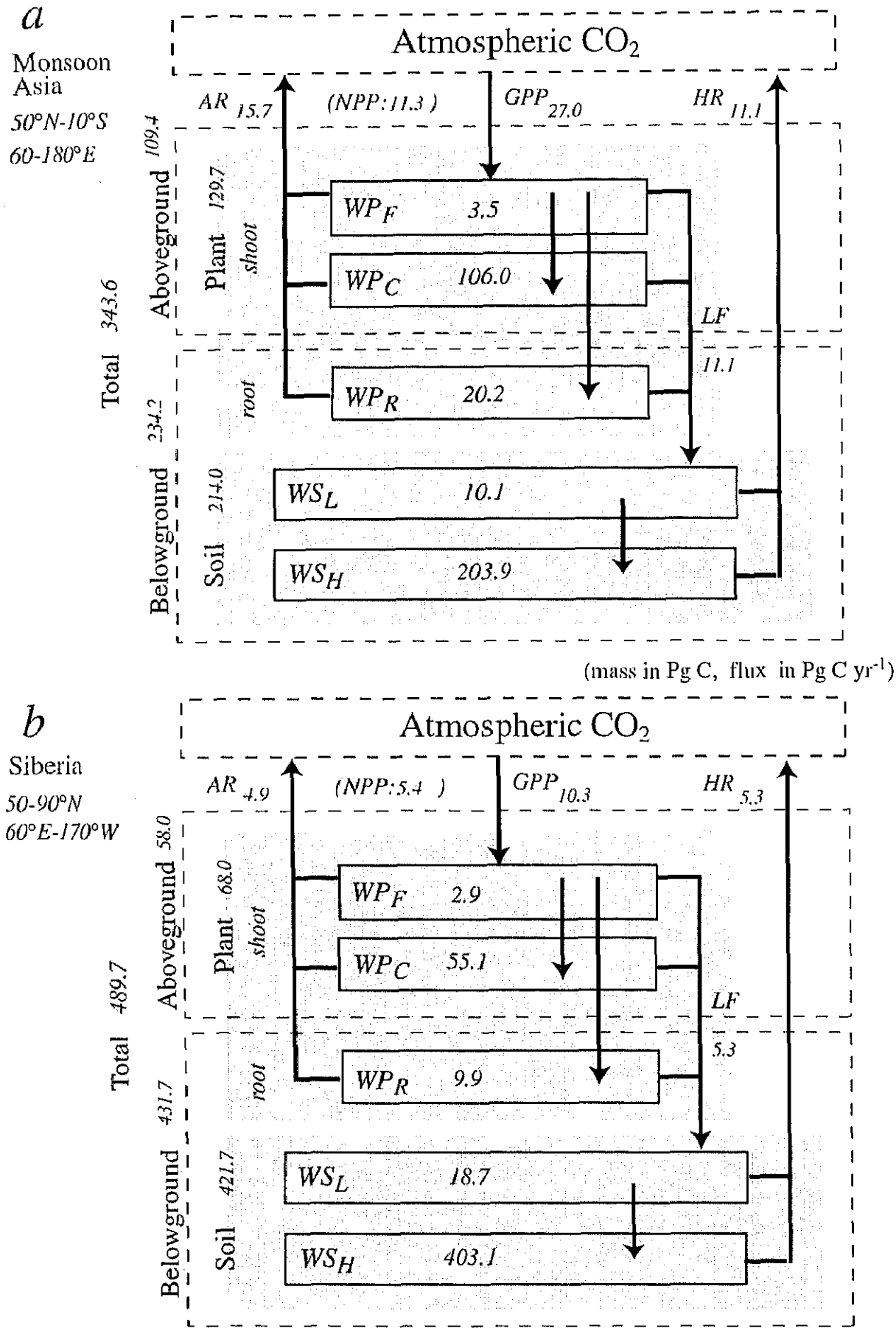

Fig. 4-16. Biospheric carbon dynamics estimated by Sim-CYCLE equilibrium run, for (a) Monsoon Asia region, and (b) Siberia region.

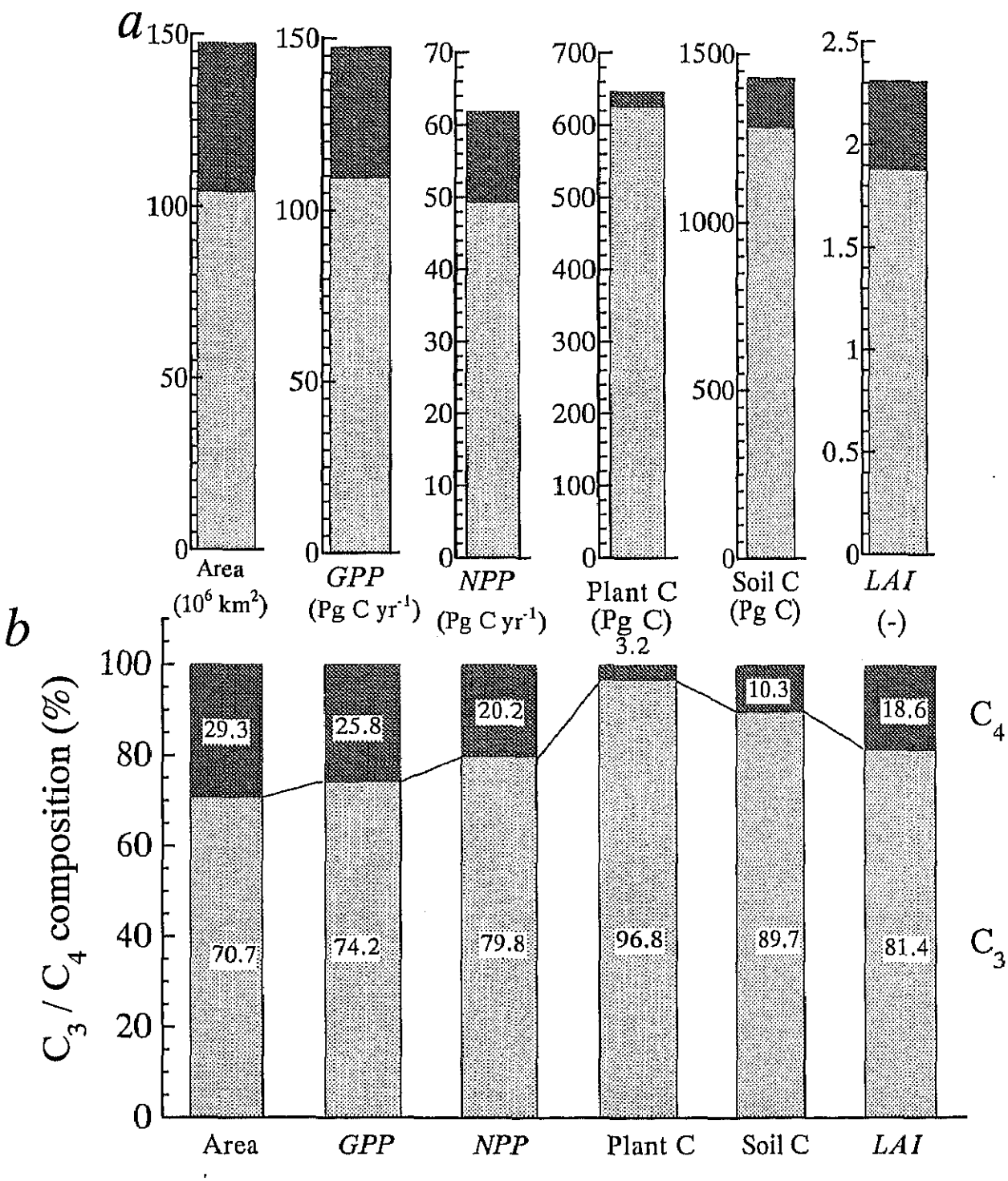

Fig. 4-17. Composition of C_3 and C_4 plants in the biospheric carbon dynamics: area, *GPP*, *NPP*, plant and Soil C storage, and *LAI* . (a) Bulk values, and (b) percents.

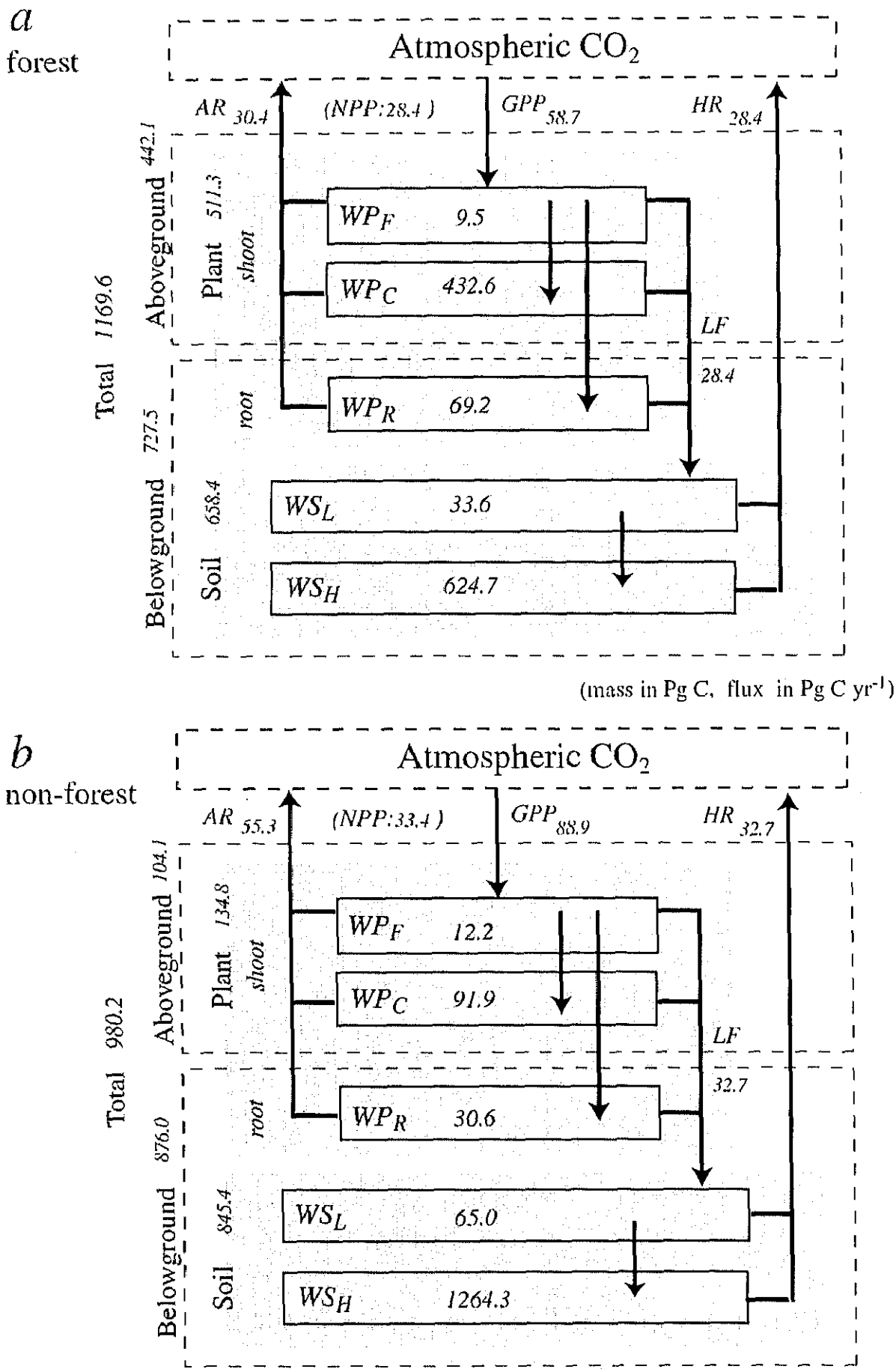

Fig. 4-18. Biospheric carbon dynamics estimated by Sim-CYCLE equilibrium run, for (a) forests, and (b) non-forest biomes.

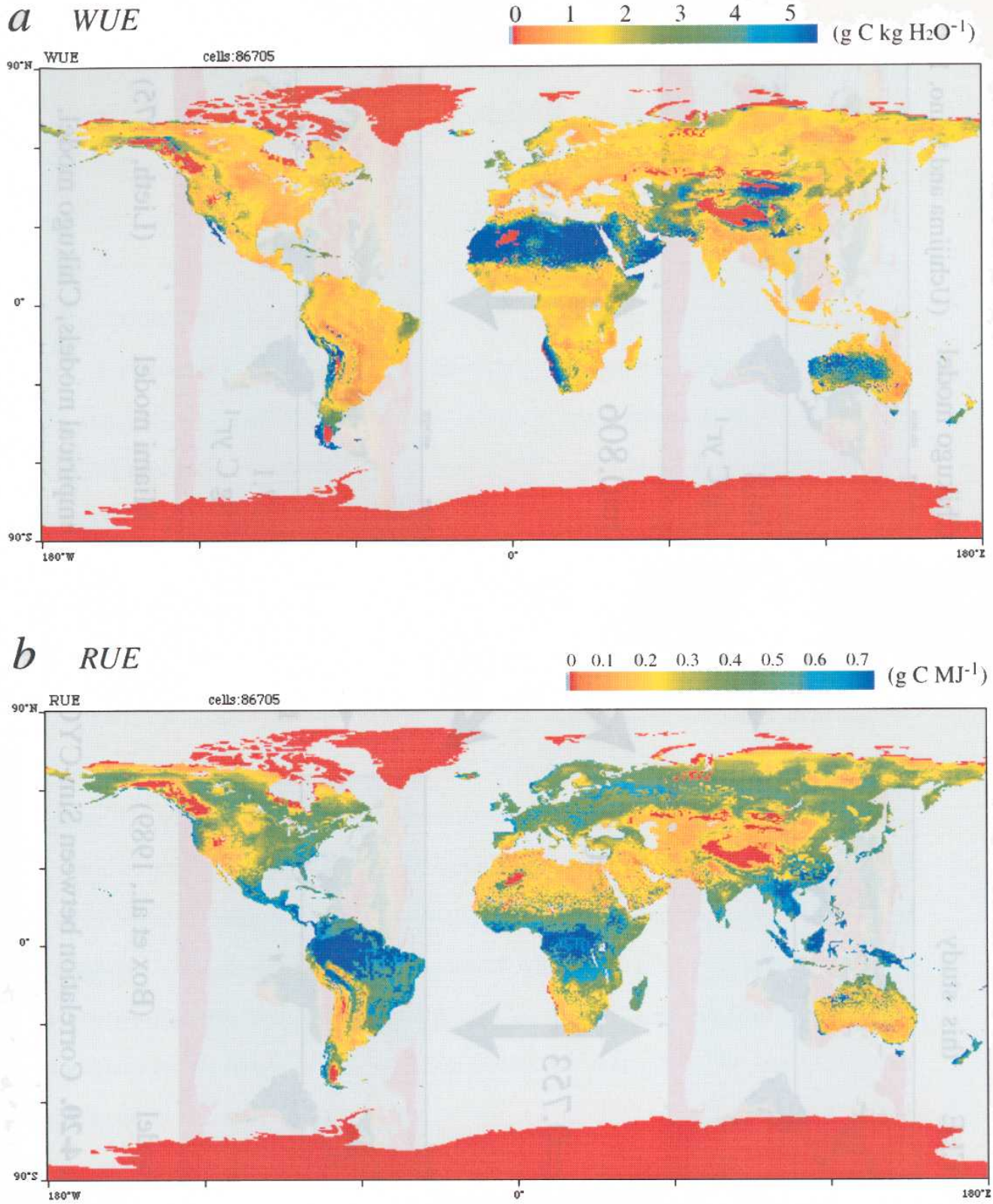

Fig.4-19. Efficiencies of photosynthetic dry-matter production, estimated by Sim-CYCLE equilibrium run. (a) Annual water use efficiency *WUE*, defined as *NPP/TR*, and (b) annual radiation use efficiency *RUE*, defined as *NPP*/absorbed PAR.

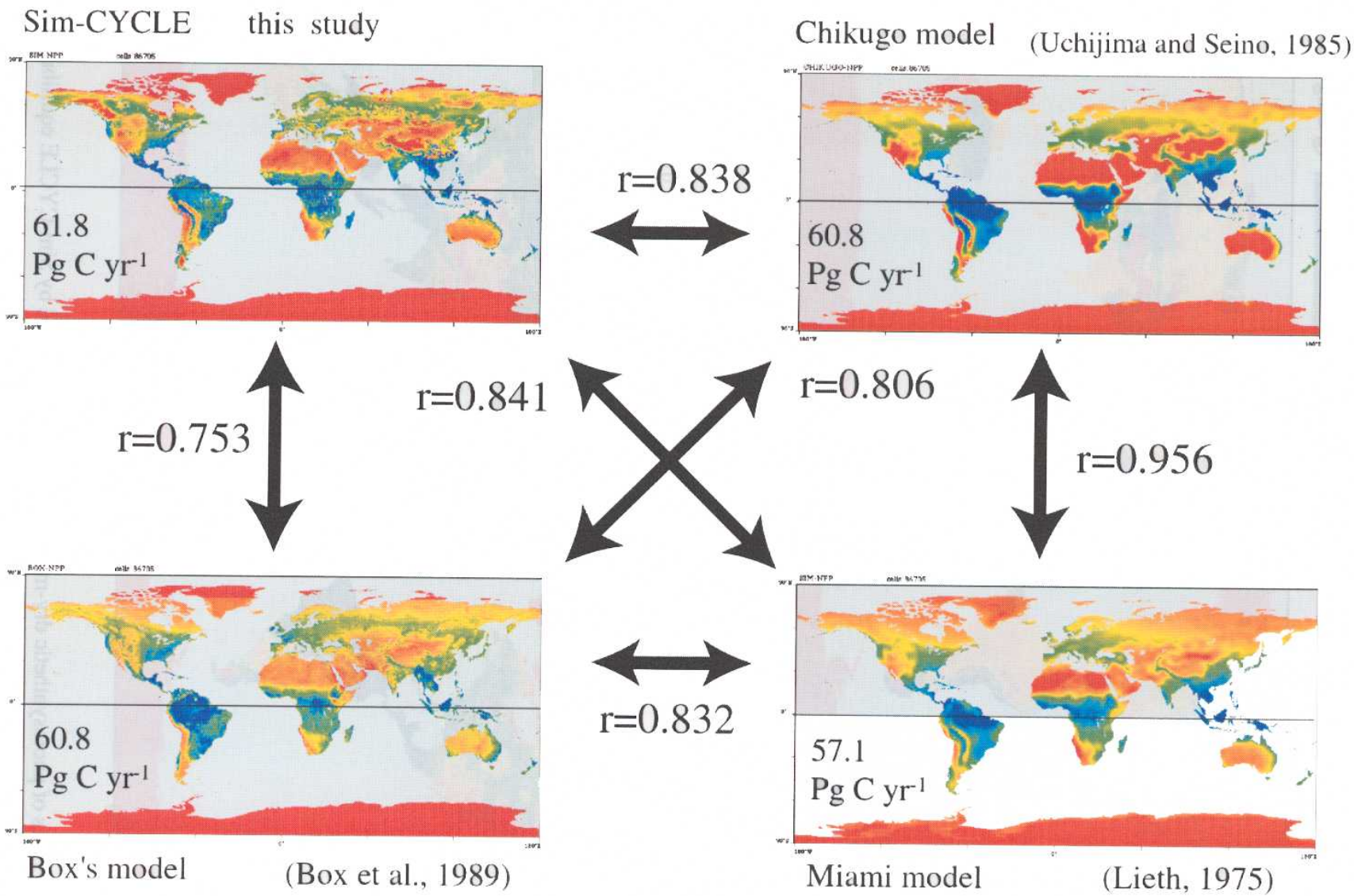

Fig. 4-20. Correlation between Sim-CYCLE and three empirical models, Chikugo model, Box's model, and Miami model, with respect to annual *NPP* distribution.